

Identifying the Complete Correlation Structure in Large-Scale High-Dimensional Data Sets with Local False Discovery Rates

Martin Gözl, Tanuj Hasija, Michael Muma and Abdelhak M. Zoubir

Abstract

The identification of the dependent components in multiple data sets is a fundamental problem in many practical applications. The challenge in these applications is that often the data sets are high-dimensional with few observations or available samples and contain latent components with unknown probability distributions. A novel mathematical formulation of this problem is proposed, which enables the inference of the underlying correlation structure with strict false positive control. In particular, the false discovery rate is controlled at a pre-defined threshold on two levels simultaneously. The deployed test statistics originate in the sample coherence matrix. The required probability models are learned from the data using the bootstrap. Local false discovery rates are used to solve the multiple hypothesis testing problem. Compared to the existing techniques in the literature, the developed technique does not assume an a priori correlation structure and work well when the number of data sets is large while the number of observations is small. The simulation results underline that it can handle the presence of distributional uncertainties, heavy-tailed noise, and outliers.

Index Terms

correlation structure, correlated subspace, multiple hypothesis testing, false discovery rate, bootstrap, small sample support

I. NOTATION

Italic normal font letters a and A denote deterministic scalar quantities. Deterministic vectors and matrices are represented by bold italic \mathbf{a} and \mathbf{A} , respectively. Upright A , \mathbf{a} and \mathbf{A} symbolize random variables, vectors and matrices, respectively. $f_A(a)$, $F_A(a)$ denote the probability density function (PDF) and cumulative distribution function (CDF) of random variable A in dependence its realization a ; $E[A]$ is its expected value. We write $g(A)$ for a generic function of A . Calligraphic \mathcal{A} denotes an arbitrary set with complement $\bar{\mathcal{A}}$ and $[A]$ is the set of non-negative integers $1, \dots, A$. Multiletter abbreviations representing mathematical quantities come sans-serif, e.g.

This research was supported by the German Research Foundation (DFG) under grants SCHR 1384/3-2 and ZO 215/17-2

M. Gözl and A. M. Zoubir are with the Signal Processing Group, TU Darmstadt, Germany. T. Hasija is with the Signal and Systems Group, Paderborn University, Germany. Michael Muma is with the Robust Data Science Group, TU Darmstadt, Germany.
corresponding author e-mail: goelz@spg.tu-darmstadt.de

FDR. The indicator function is $\mathbb{1}\{\cdot\}$. We write $\|\mathbf{a}\|$ for the Euclidean norm of \mathbf{a} and $\text{diag}(\mathbf{a})$ is a diagonal matrix with the elements of \mathbf{a} on its main diagonal. \hat{a} denotes both, the estimator and a sample estimate of a .

II. PROBLEM FORMULATION

A. System Model

We consider K data sets which are composed of zero-mean, real-valued random *observation vectors* $\{\mathbf{x}_k\}_{k \in [K]}$. For notational simplicity, we assume that all observation vectors contain an equal number I of *observations* or *subjects* $x_k^{(i)}$, such that $\mathbf{x}_k = [x_k^{(1)}, \dots, x_k^{(I)}]^\top \forall k \in [K]$. The observation vectors are assumed to be generated by the linear mixing of the latent *component vectors* $\{\mathbf{s}_k\}_{k \in [K]} \in \mathbb{R}^J$. The component vectors each contain $J \leq I$ *components*. The j th component of data set k is denoted by $s_k^{(j)}$. The relation between the observations and components is hence

$$\underbrace{\begin{bmatrix} x_k^{(1)} \\ \vdots \\ x_k^{(I)} \end{bmatrix}}_{\mathbf{x}_k} = \underbrace{\begin{bmatrix} a_k^{(1,1)} & \dots & a_k^{(1,J)} \\ \vdots & \ddots & \vdots \\ a_k^{(I,1)} & \dots & a_k^{(I,J)} \end{bmatrix}}_{\mathbf{A}_k} \cdot \underbrace{\begin{bmatrix} s_k^{(1)} \\ \vdots \\ s_k^{(J)} \end{bmatrix}}_{\mathbf{s}_k}, \quad k \in [K], \quad (1)$$

where $\mathbf{A}_k \in \mathbb{R}^{I \times J}$ is an unknown deterministic mixing matrix with full column rank. Without loss of generality, the components are assumed to be zero-mean and unit variance, i.e.,

$$\mathbb{E}[s_k^{(j)}] = 0, \quad \text{and} \quad (2)$$

$$\mathbb{E}[s_k^{(j)2}] = 1, \quad \forall k \in [K], j \in [J]. \quad (3)$$

For each $k \in [K]$, we observe N I -dimensional independent and identically distributed (i.i.d.) realizations of \mathbf{x}_k that we also refer to as the *observation samples* $\mathbf{x}_{k,1}, \dots, \mathbf{x}_{k,N}$, where $\mathbf{x}_{k,n} = [x_{k,n}^{(1)}, \dots, x_{k,n}^{(I)}]^\top$. These are summarized in the k th $I \times N$ *observation matrix* $\mathbf{X}_k = [\mathbf{x}_{k,1} \dots \mathbf{x}_{k,N}]$. The in practice unobservable k th $J \times N$ *component matrix* \mathbf{S}_k is defined analogously. The sample index $n \in [N]$ is consistent over the sets and components, i.e., $\mathbf{x}_{k,n}, \mathbf{s}_{k,n}, \mathbf{x}_{k',n}$ and $\mathbf{s}_{k',n}$ denote the paired realizations of random vectors $\mathbf{x}_k, \mathbf{s}_k, \mathbf{x}_{k'}$, and $\mathbf{s}_{k'}$ for $k, k' \in [K]$. Hence, the sample-based equivalent to Eq. (1) is

$$\underbrace{\begin{bmatrix} x_{k,1}^{(1)} & \dots & x_{k,N}^{(1)} \\ \vdots & \ddots & \vdots \\ x_{k,1}^{(I)} & \dots & x_{k,N}^{(I)} \end{bmatrix}}_{\mathbf{X}_k} = \underbrace{\begin{bmatrix} a_k^{(1,1)} & \dots & a_k^{(1,J)} \\ \vdots & \ddots & \vdots \\ a_k^{(I,1)} & \dots & a_k^{(I,J)} \end{bmatrix}}_{\mathbf{A}_k} \cdot \underbrace{\begin{bmatrix} s_{k,1}^{(1)} & \dots & s_{k,N}^{(1)} \\ \vdots & \ddots & \vdots \\ s_{k,1}^{(J)} & \dots & s_{k,N}^{(J)} \end{bmatrix}}_{\mathbf{S}_k}, \quad k \in [K]. \quad (4)$$

B. Underlying correlation structure

The observation vectors \mathbf{x}_k are the result of a linear combination of the underlying components. In practice, the observations are the outcome of the interaction between the different physical processes $\{s_k^{(j)}\}_{j \in [J]}$ with an environment described by \mathbf{A}_k . The correlation structure between the underlying source components of different

data sets defines the degree to which the observations in different sets originate in the same cause. Mathematically, this structure can be expressed using the component cross-covariance matrix between data sets $k, k' \in [K]$

$$\mathbf{R}_{\mathbf{s}_k \mathbf{s}_{k'}} = \mathbb{E} \left[\mathbf{s}_k \mathbf{s}_{k'}^\top \right] \quad (5)$$

The entry at position $(j, j') \in [J] \times [J]$ of $\mathbf{R}_{\mathbf{s}_k \mathbf{s}_{k'}}$ is the correlation coefficient $\rho_{k, k'}^{(j, j')}$ between the j th component of set k and the j' th component of set k' . If $\rho_{k, k'}^{(j, j')} \neq 0$, the j th component of set k is (partially) driven by the same underlying physical phenomenon as the j' th component of set k' .

We impose the following assumptions to facilitate the learning of the structure of the latent components from the observations.

I) Intrasets independence: the components are uncorrelated *within* each set, i.e.,

$$\mathbf{R}_{\mathbf{s}_k \mathbf{s}_k} = \mathbb{E} \left[\mathbf{s}_k \mathbf{s}_k^\top \right] = \mathbf{I}_{J \times J}, \quad (6)$$

where $\mathbf{I}_{J \times J}$ is the $J \times J$ identity matrix. This is a mild assumption: If there exists correlation between the components of a data set, those can be summarized as a single component that absorbs all components that are correlated within the set. Naturally, this reduces the dimension J of the component vector.

II) Pairwise intersets dependence: the components between any two data sets k, k' may only be correlated pairwise. Thus, component $s_{k'}^{(j)}$ may correlate with component $s_k^{(j)}$, but not with $s_{k'}^{(j')}$, $j \neq j'$. This implies that the component cross-covariance matrix between data sets k and $k' \forall k, k' \in [K] : k \neq k'$ is diagonal,

$$\mathbf{R}_{\mathbf{s}_k \mathbf{s}_{k'}} = \text{diag} \left(\left[\rho_{k, k'}^{(1)}, \rho_{k, k'}^{(2)}, \dots, \rho_{k, k'}^{(J)} \right] \right), \quad (7)$$

where we use $\rho_{k, k'}^{(j)} \equiv \rho_{k, k'}^{(j, j)}$ for readability. This assumption is common place in the literature on correlation analysis for multiple data sets, see [1] and the references therein. To the best of our knowledge, all existing methods to extract the correlation structure between multiple sets require this assumption.

III) The correlations are transitive. Hence, if $\rho_{k, k'}^{(j)} > 0$ and $\rho_{k', k''}^{(j)} > 0$, then also $\rho_{k, k''}^{(j)} > 0 \forall k, k', k'' \in [K]$.

The correlation structure is fully specified by the correlation coefficients $\rho_{k, k'}^{(j)}, \forall j \in [J]$ on the main diagonal of the correlation matrices $\mathbf{R}_{\mathbf{s}_k \mathbf{s}_{k'}}, k, k' \in [K], k \neq k'$, since the off-diagonal entries are all zero due to Assumption II) and $\mathbf{R}_{\mathbf{s}_k \mathbf{s}_k}$ is identity according to Assumption I. We define the $J \times K$ *activation matrix*

$$\mathbf{M} = \begin{bmatrix} M_1^{(1)} & \dots & M_K^{(1)} \\ \vdots & \ddots & \vdots \\ M_1^{(J)} & \dots & M_K^{(J)} \end{bmatrix} \quad (8)$$

to indicate which components are correlated across which data sets. If the j th component is correlated between data set $k \in [K]$ and at least one other data set $k' \in [K] : k \neq k'$, i.e., $\exists \rho_{k, k'}^{(j)} > 0$, then $M_k^{(j)} = M_{k'}^{(j)} = 1$. Otherwise, $M_k^{(j)} = 0$. Thus, either $\sum_{k=1}^K M_k^{(j)} \geq 2$ or $\sum_{k=1}^K M_k^{(j)} = 0$. We write $\bar{\mathcal{K}}^{(j)}, j \in [J]$ to denote the collection of those sets whose j th component is correlated. Its complement is $\mathcal{K}^{(j)}$. If all $\mathbf{R}_{\mathbf{s}_k \mathbf{s}_{k'}}, \forall k, k' \in [K]$ were observable, \mathbf{M} could be deduced directly from their non-zero elements. We illustrate the relation between the assumptions, the correlation matrices and the activation matrix by a low-dimensional example with $K = 4$ data sets in Fig. 1.

j	$\rho_{1,2}^{(j)}$	$\rho_{1,3}^{(j)}$	$\rho_{1,4}^{(j)}$	$\rho_{2,3}^{(j)}$	$\rho_{2,4}^{(j)}$	$\rho_{3,4}^{(j)}$
1	.7	.8	.8	.7	.8	.9
2	.9	0	.75	0	.8	0
3	0	0	0	.9	0	0
4	0	.4	.35	0	0	.4
5	0	0	0	.5	0	0
6	0	0	0	0	0	0
7	0	0	0	0	0	0

\iff

$M = \begin{bmatrix} 1 & 1 & 1 & 1 \\ 1 & 1 & 0 & 1 \\ 0 & 1 & 1 & 0 \\ 1 & 0 & 1 & 1 \\ 0 & 1 & 1 & 0 \\ 0 & 0 & 0 & 0 \\ 0 & 0 & 0 & 0 \end{bmatrix}$

Figure 1: An example with $K = 4$ data sets and 7 components per set. The correlation coefficients are given in the table on the left and the corresponding activation matrix is shown on the right. Such correlation structures arise in a large number of practical applications. For instance, the different data sets may correspond to recordings by different cameras that are deployed in different locations. The components may then be the visual signatures of different visual objects and identifying correlated components may then help to track the movement of a certain object across the surveillance area. In environmental monitoring, each data set may correspond to the measurements obtained with a sensor that records multiple environmental measures such as temperature, humidity or pollution. The components could then correspond to different meteorological or man-made phenomena and knowing the correlation structure across different sensors would be useful in both, identifying the presence of such underlying phenomena and localizing the areas which they affect.

Remark on the component indices: The methods discussed in this work assume that the "absolute" index $j \in [J]$ of a component is of limited interest. The covered procedures generally assume that the components are sorted such that component with index $j = 1$ exhibits the strongest correlation across all data sets and with $j = J$ the weakest. This is well-justified in practical applications where the underlying component and mixing matrices are typically unknown and the absolute ordering of rows of \mathbf{A}_k and columns of \mathbf{S}_k does not play a role.

III. CORRELATION STRUCTURE ESTIMATION BASED ON THE COHERENCE MATRIX

We intend to identify the unknown structure between the latent components across the different data sets. In practice, \mathbf{M} is not directly observable and must be estimated based on the sample-based model given in Eq. (4). We denote its estimate by $\widehat{\mathbf{M}}$, with entries $\widehat{M}_k^{(j)}$. The problem of estimating \mathbf{M} was first considered in [1]. The multiple testing procedure proposed in this work utilizes some of the theoretical findings from [1]. Hence, we summarize the procedure developed in [1] in what follows.

A. The two-step procedure (TSP) [1]

The number of components that are correlated across at least two data sets be denoted by $D \leq J$. D is equivalent to the total number of rows in \mathbf{M} with at least two non-zero elements. The TSP from [1] bases upon the eigenvalues

and eigenvectors of the so-called *composite coherence matrix*

$$\mathbf{C} = \mathbf{R}_D^{-\frac{1}{2}} \mathbf{R} \mathbf{R}_D^{-\frac{1}{2}} = \mathbf{R}_D^{-\frac{1}{2}} \cdot \mathbb{E} \left[\left[\mathbf{x}_1^\top, \dots, \mathbf{x}_K^\top \right]^\top \cdot \left[\mathbf{x}_1^\top, \dots, \mathbf{x}_K^\top \right] \right] \cdot \mathbf{R}_D^{-\frac{1}{2}}. \quad (9)$$

$\mathbf{R}_D = \text{blkdiag}(\mathbf{R}_{\mathbf{x}_1 \mathbf{x}_1}, \dots, \mathbf{R}_{\mathbf{x}_K \mathbf{x}_K})$ is block-diagonal with blocks $\mathbf{R}_{\mathbf{x}_k \mathbf{x}_k} = \mathbb{E}[\mathbf{x}_k \mathbf{x}_k^\top]$ and $(\cdot)^{-\frac{1}{2}}$ denotes the inverse of the matrix square root.

The eigenvalues of \mathbf{C} sorted in descending order be denoted by $\lambda^{(1)}, \dots, \lambda^{(JK)}$ with corresponding eigenvectors $\mathbf{u}^{(1)}, \dots, \mathbf{u}^{(JK)}$. A series of theorems in [1] proves that under certain conditions, exactly one out of the K eigenvalues associated with the j th correlated component is greater than 1, $j \in [D]$. The remaining $K-1$ eigenvalues of component $j \in [D]$ are all ≤ 1 . For the j th component $D < j \leq J$ that is uncorrelated across all K data sets, all associated eigenvalues are equal to 1. In total, exactly D eigenvalues of \mathbf{C} are greater than 1. Hence, the correlation structure analysis in [1] focuses exclusively on the largest J eigenvalues $\lambda^{(j)}$ and the corresponding $J \cdot K$ -dimensional eigenvectors $\mathbf{u}^{(j)}$, $j \in [J]$. The latter can be decomposed as $\mathbf{u}^{(j)} = \left[\mathbf{u}_1^{(j)\top}, \dots, \mathbf{u}_K^{(j)\top} \right]^\top$, where the J -dimensional *eigenvector chunk* $\mathbf{u}_k^{(j)}$ summarizes the contribution of data set k to eigenvalue $\lambda^{(j)}$, $j \in [J]$. With $\mathbf{0}_J$ denoting a J -dimensional all-zero vector, the following has been shown about the eigenvector chunks [1]:

$$\mathbf{u}_k^{(j)} \begin{cases} = \mathbf{0}_J, & \text{if } j \in [D] \text{ and } k \in \overline{\mathcal{K}}^{(j)}, \text{ i.e., the } j\text{th component is correlated between set } k \text{ and another set,} \\ \neq \mathbf{0}_J, & \text{if } j \in [D] \text{ and } k \in \mathcal{K}^{(j)}, \text{ i.e., the } j\text{th component is not correlated between set } k \text{ and any other set.} \end{cases} \quad (10)$$

This property of the coherence matrix eigenvector chunks has lead to a two-step procedure for identifying correlations across sets in [1].

- I) Find all D eigenvalues of \mathbf{C} for which $\lambda^{(j)} > 1$, $j \in [D]$ and set $M_k^{(j)} = 0 \forall j > D, k \in [K]$.
- II) The remaining entries of \mathbf{M} are found with $M_k^{(j)} = \mathbb{1} \left\{ \left\| \mathbf{u}_k^{(j)} \right\|^2 > 0 \right\}$, $\forall j \in [D], k \in [K]$.

In practice, \mathbf{C} is unknown and has to be estimated from the data $\mathbf{X}_k, k \in [K]$. The estimate $\widehat{\mathbf{C}}$ [1] is a random matrix. The sample covariance matrix is deployed to estimate the quantities in Eq. (9),

$$\widehat{\mathbf{R}}_D = \text{blkdiag}(\widehat{\mathbf{R}}_{\mathbf{x}_1 \mathbf{x}_1}, \dots, \widehat{\mathbf{R}}_{\mathbf{x}_K \mathbf{x}_K}), \quad (11)$$

$$\widehat{\mathbf{R}}_{\mathbf{x}_k \mathbf{x}_k} = \frac{1}{N} \sum_{n=1}^N \mathbf{x}_{k,n} \mathbf{x}_{k,n}^\top, \quad (12)$$

$$\widehat{\mathbf{R}} = \frac{1}{N} \sum_{n=1}^N \left[\mathbf{x}_{1,n}^\top, \dots, \mathbf{x}_{K,n}^\top \right]^\top \cdot \left[\mathbf{x}_{1,n}^\top, \dots, \mathbf{x}_{K,n}^\top \right]. \quad (13)$$

The eigenvalues $\widehat{\lambda}^{(j)}$ and eigenvectors $\widehat{\mathbf{u}}^{(j)}$ of $\widehat{\mathbf{C}}$ are random variables and vectors, respectively. As a consequence, neither the eigenvalues of \mathbf{C} associated with uncorrelated components are strictly ≤ 1 , nor are the chunk norms $\left\| \widehat{\mathbf{u}}_k^{(j)} \right\|^2, j \in [D]$ exactly equal to 0 if $k \in \mathcal{K}^{(j)}$. Instead, the eigenvalues and eigenvector chunk norms follow PDFs $f_{\widehat{\lambda}^{(j)}}(\lambda)$ and $f_{\widehat{\mathbf{u}}_k^{(j)}}(\mathbf{u})$. To infer the correlation structure from those random quantities, the authors of [1] propose to formulate both steps as separate hypothesis testing problems.

Step I: By iterating over $d \in [J]$, perform a series of binary tests between the d total correlations null hypothesis ${}_I H^{(d)}$ and the d total correlations alternative ${}_I \bar{H}^{(d)}$ where

$${}_I H^{(d)} : \quad d = D, \quad \text{i.e., there are exactly } d \text{ components with non-zero inter-set correlation,} \quad (14)$$

$${}_I \bar{H}^{(d)} : \quad d > D, \quad \text{i.e., there are more than } d \text{ components with non-zero inter-set correlation.} \quad (15)$$

The decisions between ${}_I H^{(d)}$ and ${}_I \bar{H}^{(d)}$ are based on test statistics $T^{(d)} = g(\hat{\lambda}^{(1)}, \dots, \hat{\lambda}^{(d)})$, where $g : d \rightarrow 1$ is a function of the d largest eigenvalues of $\hat{\mathbf{C}}$ [1]. The test statistic PDF and CDF under the d th component number null hypothesis ${}_I H^{(d)}$ be denoted by $f_{T^{(d)}|{}_I H^{(d)}}(t)$ and $F_{T^{(d)}|{}_I H^{(d)}}(t)$. The decisions between ${}_I H^{(d)}$ and ${}_I \bar{H}^{(d)}$ are made by thresholding the total correlations p -value $p^{(d)}$ at false alarm level ${}_I \alpha_{\text{FA}}$, i.e.,

$$\int_{T^{(d)}}^{\infty} f_{T^{(d)}|{}_I H^{(d)}}(t) dt = p^{(d)} \underset{{}_I \bar{H}^{(d)}}{\overset{{}_I H^{(d)}}{\geq}} {}_I \alpha_{\text{FA}}. \quad (16)$$

If ${}_I H^{(d)}$ the estimated number of correlated sources is $\hat{D} = d$. Hence, set $\hat{M}_k^{(j)} = 0, \forall j \in \{\hat{D} + 1, \dots, J\}, k \in [K]$.

Step II: Given \hat{D} from Step I) such that $\hat{D} \leq D$, define a set of K binary hypotheses for each $j \in [\hat{D}]$,

$${}_{II} H_k^{(j)} : \quad k \in \mathcal{K}^{(j)} : \text{The } j\text{th component is uncorrelated between the sets } k, k', \forall k' \in [K], k \neq k', \quad (17)$$

$${}_{II} \bar{H}_k^{(j)} : \quad k \in \bar{\mathcal{K}}^{(j)} : \exists k' \in [K], k \neq k' \text{ s.t. the } j\text{th component is correlated between the sets } k \text{ and } k'. \quad (18)$$

We refer to ${}_{II} H_k^{(j)}$ and ${}_{II} \bar{H}_k^{(j)}$ as the set-wise j th component null hypothesis and set-wise j th component alternative, respectively. As test statistics, the norms of the estimated eigenvector chunks $c_k^{(j)} = \|\hat{\mathbf{u}}_k^{(j)}\|^2$ are deployed. Under the set-wise component null hypothesis, the test statistic PDF is $f_{c_k^{(j)}|{}_{II} H_k^{(j)}}(c)$. The decisions between the ${}_{II} H_k^{(j)}$ and ${}_{II} \bar{H}_k^{(j)}$ are made by thresholding the set-wise component p -values $p_k^{(j)}$, i.e.,

$$\int_{c_k^{(j)}}^{\infty} f_{c_k^{(j)}|{}_{II} H_k^{(j)}}(c) dc = p_k^{(j)} \underset{{}_{II} \bar{H}_k^{(j)}}{\overset{{}_{II} H_k^{(j)}}{\geq}} {}_{II} \alpha_{\text{FA}}. \quad (19)$$

with the user-defined Step II false alarm probability level ${}_{II} \alpha_{\text{FA}}$. If ${}_{II} H_k^{(j)}$ is accepted, then $\hat{M}_k^{(j)} = 0$. Otherwise, $\hat{M}_k^{(j)} = 1$. This completes the TSP estimator of \mathbf{M} .

IV. THE PROPOSED ONE-STEP PROCEDURE WITH FALSE POSITIVE CONTROL

In this section, we propose a novel holistic approach to estimating the activation matrix \mathbf{M} . We first motivate this approach by highlighting the benefits of a single detection step over the state-of-the art TSP from [1]. We then provide the required theory with a particular focus on the false positive control properties of the proposed one-step procedure (OSP).

A. Motivation

A TSP to identifying the complete correlation structure between components from multiple data sets like the one from [1] exhibits two major problems. Firstly, false alarms are controlled in both steps individually, but not for the combination of the two steps. Secondly, controlling the false alarm probability is not well-suited to limit false positives when many binary hypothesis tests are performed simultaneously. In what follows, we discuss those issues in detail and propose solutions that form the basis of the proposed OSP.

1) *Error propagation*: The TSP attempts to control the false positives in both steps independently by thresholding the respective p -values at nominal false alarm levels ${}_I\alpha_{FA}$ and ${}_{II}\alpha_{FA}$ in Eqs. (14), (17). However, the false positives are not controlled for the sequential combination of these two steps. The method proposed in [1, Theorem 1] infers that a data set k belongs to the collection of correlated sets $\bar{\mathcal{K}}^{(j)}$ of the j th component, if the corresponding eigenvector chunk norm $c_k^{(j)} = \|\hat{\mathbf{u}}_k^{(j)}\|^2$ is significantly non-zero, since $\|\mathbf{u}_k^{(j)}\|^2 \neq 0$ if $k \in \bar{\mathcal{K}}^{(j)}$ and $\|\mathbf{u}_k^{(j)}\|^2 = 0$ otherwise. However, this assumption does not hold if the j th component is uncorrelated across all sets. Since ${}_I\alpha_{FA} > 0$, false alarms can occur in Step I. If Step I concludes with a false alarm, the number of components with correlation between at least two sets is overestimated, $\hat{D} > D$. Then, the chunk norms associated with the j th component, $D < j \leq \hat{D}$ all are significantly non-zero and the tests in Step II are based on wrong assumptions. The heatmap in Fig. 2a shows the average chunk norm value obtained for the toy example introduced previously in Fig. 1, with $N = 500$ realizations of Gaussian distributed component and noise vectors. The signal-to-noise ratio (SNR) is 5dB. Since $D = 5$, the sixth and seventh component are entirely uncorrelated. However, the average chunk norms in the sixth and seventh row are far from zero. Instead, their values are similar to those of the first component, which is correlated across all sets. In addition, the empirical distribution functions (EDFs) of the p -values for Step II are provided for some components and sets in Fig. 2b. If the j th component of set k is uncorrelated with the other sets, the p -values should closely follow a uniform distribution $\mathcal{U}(0, 1)$ to guarantee that the false alarm probability is bounded by the nominal level ${}_{II}\alpha_{FA}$. The nominal false alarm level is fulfilled for the j th components, $j \in D$, since the p -value distribution is approximately uniform in the typical $[0, .2]$ range of ${}_{II}\alpha_{FA}$. As an example, we provide the EDF for the second component and the third set on the top left of Fig. 2b. On the top right, the EDF of the p -values for the fourth component of set $k = 1$ is shown, which is correlated with the fourth component of the third and the fourth set. Here, a lot of mass is located close to zero, making it highly likely to discover the correlation. The second row of Fig. 2b shows some p -value distributions obtained for the sixth and seven component, which are uncorrelated across all sets. Nevertheless, these EDFs look very similar to the one on the top right. Hence, falsely identifying correlation is much more likely than the nominal false alarm level ${}_{II}\alpha_{FA}$. The statistical behavior of the chunk norms $\hat{\mathbf{u}}_k^{(j)}$ for $D < j$ is similar to that of chunk norms of components which are correlated across all data sets. Hence, overestimation of $\hat{D} > D$ leads to uncontrolled false alarm probabilities in Step II).

A different problem arises if Step I terminates with a Type II error, i.e., a decision in favor of ${}_I H^{(d)}$ while $d < D$. Then, regardless of the information contained in the eigenvector chunks, no correlations can be identified for the j th components of any data sets, $\hat{D} < j \leq D$. A potentially significant amount of true correlations remain unidentified even if the eigenvector chunks contain strong evidence in favor of additional correlated components. This is illustrated in Fig. 3. In this example, $D = 6$ out of $J = 10$ components are correlated across 7, 6, 5, 4, 3 and 2 out of $K = 15$ data sets with correlation coefficients .7, .7, .65, .6, .6, .55, respectively. $N = 300$ realizations are observed and the components and noise are Gaussian with SNR = 5dB. The correlation coefficients are constant per component, i.e., if the $j = 5$ th component is correlated across sets 1, 2 and 3, then $\rho_{1,2}^{(5)} = \rho_{2,3}^{(5)} = \rho_{1,3}^{(5)} = .6$. The results are averaged over 100 independent realizations of the experiment. The average chunk norms in Fig. 3a are again distinctly indicating the true correlation structure among the first five components. However, Step I consistently underestimates D : The average of \hat{D} is 1.67 for the reasonable false alarm level ${}_I\alpha_{FA} = .1$. Since more than half of

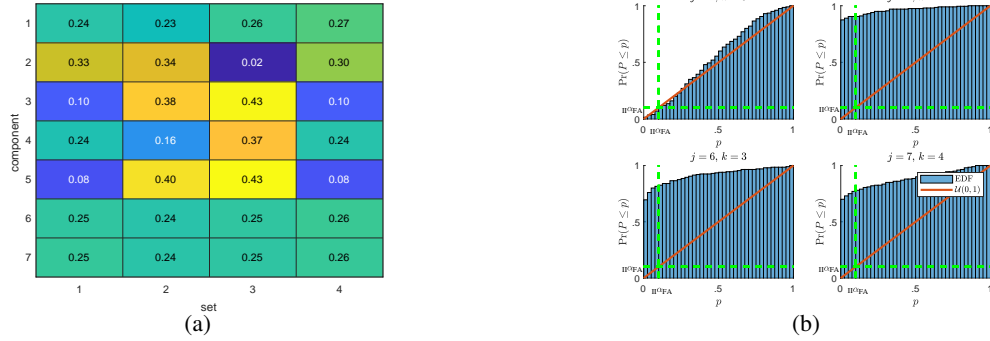


Figure 2 – (a): The average chunk norms extracted from four data sets with Gaussian components and noise, SNR = 5dB and the correlation structure given in Fig. 1. The chunk norms associated with components that are uncorrelated across all sets are far from zero, which invalidates the assumption that the chunk norms are close to zero under $\Pi H_k^{(j)}$ testing procedure in Step II of the TSP. – (b): The p -value EDFs for different sets and components. $\Pi H_k^{(j)}$ holds in the top left and since $j \leq D$, false positives can be controlled at a typical nominal level $\Pi \alpha_{FA} = .1$. The top right displays the p -value EDF under $\Pi \bar{H}_k^{(j)}$, indicating a high probability of detection. The bottom row underlines that $\Pi \alpha_{FA}$ is significantly violated if $j > D$.

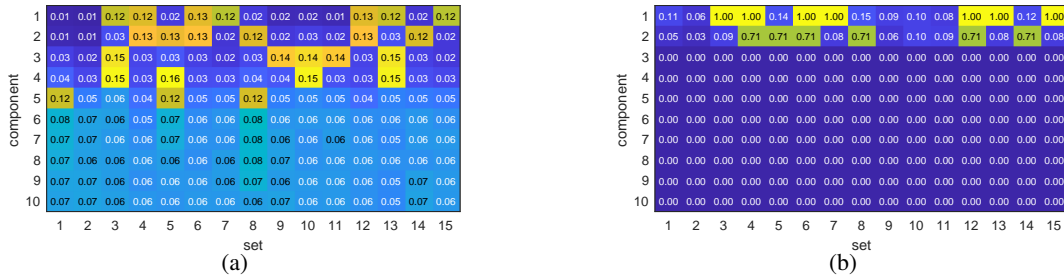


Figure 3 – (a) The average chunks norms for a scenario where the j th component is correlated across $7 - j$ sets, $j \in [D]$, $D = 6$. The strength of the correlation also decreases with increasing component index j . The chunk norms associated with sets across which the j th component is correlated are clearly visible $j \in [5]$. – (b) The detection probabilities for $\alpha_{FA} = \Pi \alpha_{FA} = .1$. Step I of the TSP yields on average a value of 1.67 for \hat{D} . No correlations beyond the second component are identified.

the true correlations occur beyond the second component, a significant percentage of true correlations is not even tested for in Step II, as the detection probabilities in Fig. 3b underline. Hence, the TSP exhibits poor detection power and a large fraction of the true correlations remain undetected, despite that the chunk norms displayed in Fig. 3a yield considerable evidence on the underlying correlation structure.

2) *False positive control*: Assume now that Step I yielded the correct number of correlated components, $\hat{D} = D$. Hence, the detector in Step II is based on test statistics $\Pi T_k^{(j)}$ for which the relations from [1, Theorem 1] hold and the false alarm probability is controlled for each test at the nominal level $\Pi \alpha_{FA}$. Step II performs in total $\hat{D} \cdot K$

binary tests between ${}_{\Pi}H_k^{(j)}$ and ${}_{\Pi}\overline{H}_k^{(j)}$, $\forall k \in [K], j \in [\hat{D}]$. Let π_0 denote the proportion of true set-wise component null hypotheses. Then, on average, $\pi_0 \cdot \hat{D} \cdot K \cdot {}_{\Pi}\alpha_{\text{FA}}$ true set-wise component null hypotheses get rejected. The fraction of true null hypotheses π_0 is unknown in practice. Thus, if Step II results in a total number of R rejections, i.e., decisions in favor of the alternative, it is impossible to assess how many of the R accepted alternatives are false positives. In fact, all R rejections could be false, despite the individual false alarm probabilities being controlled at level ${}_{\Pi}\alpha_{\text{FA}}$. A false positive corresponds to an erroneously identified correlation of components in at least two data sets. Falsely detected correlations can have a significant impact. Consider genome-wide association studies [2]. Falsely identified correlations between a genome and a bio-marker could trigger intensive follow-up research efforts. Hence, using a detector to identify interesting genomes which produces false positives in an uncontrolled manner can lead to a significant waste of resources [3].

B. Multiple hypothesis testing

Our proposed method identifies the complete correlation structure in a single step. Thus, it is not subject to the aforementioned error propagation between steps. To ensure that the identified correlations come with statistical error guarantees and are thus meaningful, we resort to multiple hypothesis testing (MHT) [4] false positive measures. The common principle in MHT is to account for the multiplicity of binary decisions by a correction of the individual test statistics. Depending on the type of correction, MHT detectors are designed to control statistical performance measures that allow to quantify the reliability of the R rejections. The two most commonly used measures are the family-wise error rate (FWER) [5] and the false discovery rate (FDR) [6]. The FWER is the probability that at least one of the R discoveries is a false positive, while the FDR is the expected fraction of false discoveries among all discoveries. Procedures that control the FWER are particularly useful for problems where already a single false positive is very costly, while a missed discovery is less critical. A missed discovery occurs, whenever a decision in favor of the null hypothesis is made while the alternative is true. If the FWER is controlled at the nominal level α , the probability that at least one of the R discovery is a false discovery is $\leq \alpha$. In contrast, controlling the FDR permits more false positives, if more correct discoveries are made: If a procedure controls the FDR at nominal level α , no more than on average $\alpha \cdot R$ discoveries are false. For correlation structure identification, limiting the probability of a single false positive appears unnecessarily strict. A small fraction of false positives among all positives is sufficient, as this allows identifying more true positives while keeping results trustworthy. Thus, we focus on controlling the FDR in this work.

C. Proposed MHT problem for correlation structure identification

We first define a set of binary hypotheses ,

$$H_k^{(j)} : \quad k \in \mathcal{K}^{(j)} : \text{The } j\text{th components of sets } k \text{ and } k' \text{ are uncorrelated, } j \in [J], k, k' \in [K], k \neq k', \quad (20)$$

$$\overline{H}_k^{(j)} : \quad k \in \overline{\mathcal{K}}^{(j)} : \text{The } j\text{th components of sets } k \text{ and } k' \text{ are correlated, } j \in [J], k, k' \in [K], k \neq k'. \quad (21)$$

We refer to $H_k^{(j)}$ and $\overline{H}_k^{(j)}$ as the atom null hypothesis and atom alternative, respectively, since an *atom* is the smallest indivisible unit. In contrast to the hypotheses defined in Eq. (17) that are used in the second step of

the TSP, the atom hypotheses do *not* depend on an estimate for the total number of correlated components D . We infer the true atom nulls and alternatives based on test statistics $T_k^{(j)} \sim f_{T_k^{(j)}}(t)$ that follow $f_{T_k^{(j)}|H_k^{(j)}}(t)$ and $f_{T_k^{(j)}|\overline{H}_k^{(j)}}(t)$ under $H_k^{(j)}$ and $\overline{H}_k^{(j)}$, respectively. The details on $T_k^{(j)}$ are provided in Sec. IV-E. Finally, the elements of the activation matrix are estimated as $\hat{M}_k^{(j)} = 0 \forall k \in [K], j \in [J]$ where $H_k^{(j)}$ is accepted and $\hat{M}_k^{(j)} = 1$ otherwise.

In addition, we define a set of binary hypotheses for the components

$$H^{(j)} : \quad \text{The } j\text{th component is uncorrelated across all sets, } j \in [J], \overline{\mathcal{K}}^{(j)} = \emptyset, \quad (22)$$

$$\overline{H}^{(j)} : \quad \text{The } j\text{th component is correlated between at least two sets } k, k' \in [K], |\overline{\mathcal{K}}^{(j)}| \geq 2, j \in [J]. \quad (23)$$

The component null hypotheses $H^{(j)}$ and component alternatives $\overline{H}^{(j)}$ are unions of their respective component's atom hypotheses: If all $H_k^{(j)} \forall k \in [K]$ hold for a $j \in [J]$, then $H^{(j)}$ holds as well.

To identify the activation matrix \mathbf{M} , the proposed OSP requires $J \cdot K$ binary tests. Be $R \leq J \cdot K$ the total number of times a decision in favor of the alternative is made, or, the number of *atom discoveries*. Naturally, $R = S + V$ with S and V the numbers of correct and false atom discoveries. R is observable, but S and V are not. Our proposed approach attempts to maximize $E[S] = \sum_{j=1}^J \sum_{k=1}^K P(\hat{M}_k^{(j)} = 1 | M_k^{(j)} = 1)$ while controlling the *atom FDR*

$$\text{FDR} = E \left[\frac{V}{R} \right], \quad (24)$$

the expected number of atom false discoveries among all atom discoveries at a nominal level α . This guarantees that on average at least $(1 - \alpha)\%$ of the non-zero elements in $\widehat{\mathbf{M}}$ correspond to true correlations.

In addition to controlling false positives on the atom-level, one may also be interested in controlling the component-level false positives. This is particularly useful if atom-level false positives differ in importance based on the corresponding component. It is often much more critical to avoid accidentally declared correlation between at least two sets for the j th component that is uncorrelated between all sets than accidentally identifying correlation for the j' th component of set k if this component is correlated between other sets, $k \notin \overline{\mathcal{K}}^{(j')} \neq \emptyset$. We denote the number of component discoveries, false discoveries and true discoveries by R_{cmp} , V_{cmp} and S_{cmp} , respectively. Then, the *component FDR* is

$$\text{FDR}_{\text{cmp}} = E \left[\frac{V_{\text{cmp}}}{R_{\text{cmp}}} \right], \quad (25)$$

which we attempt to control at the nominal level α_{cmp} .

Finally, we revisit the fact that either none or at least two atom hypotheses must be rejected per component with index $j \in [J]$, since correlation *in between* data sets is considered. This structural property has to be incorporated directly into the testing procedure to guarantee strict control of the atom FDR at level α and maximize the detection power. If it was enforced only *after* the hypothesis testing procedure has been applied, i.e., by a posteriori accepting the atom null hypothesis $H^{(j)}$ for all atoms of components $j \in [J]$ where $\sum_{k=1}^K \hat{M}_k^{(j)} = |\overline{\mathcal{K}}^{(j)}| = 1$, FDR control is lost. If $|\overline{\mathcal{K}}^{(j)}| = 1$ due to missed detection(s), i.e., if the actual number of sets across which the j th component is correlated is ≥ 2 , this posterior cleaning reduces the number of correct positives, thereby increasing the FDR. In addition, if $|\overline{\mathcal{K}}^{(j)}| = 1$ while the j th component is uncorrelated across all sets, then the final FDR is smaller than with the results of the FDR control procedure and additional discoveries may have been possible.

The complete MHT-based correlation structure identification problem is, hence,

$$\begin{aligned} \widehat{\mathbf{M}}_{\text{MHT}} &= \underset{\widehat{\mathbf{M}}}{\operatorname{argmax}} \sum_{j=1}^J \sum_{k=1}^K P(\widehat{M}_k^{(j)} = 1 | M_k^{(j)} = 1), \\ \text{s.t.} \quad & \text{FDR} \leq \alpha, \\ & \text{FDR}_{\text{cmp}} \leq \alpha_{\text{cmp}}, \\ & \left(\sum_{k=1}^K \widehat{M}_k^{(j)} \right) \neq 1, \forall j \in [J]. \end{aligned} \quad (26)$$

D. Proposed empirical Bayes solution

Eq. (26) is a very challenging MHT problem. To the best of our knowledge, a solution does not yet exist in the open literature. The well-known Benjamini-Hochberg procedure (BH) [6], for instance, which computes a p -value for each tested null hypothesis and then rank-order the p -values to identify those that indicate little support for their associated null hypotheses does neither maximize detection power, nor does it provide control on multiple FDRs simultaneously, nor can it fulfill structural conditions.

We resort to MHT with local false discovery rates (lfdrs) [3], [7]. The lfdr is the empirical Bayes probability for a null hypothesis to hold, given the observed data. In what follows, we design a probability-based MHT approach to solving Eq. (26).

The atom lfdrs are

$$P(H_k^{(j)} | \mathcal{P}) = \text{lfdr}_k^{(j)} \equiv \text{lfdr}(p_k^{(j)}) = \frac{\pi_0}{f_P(p_k^{(j)})}, \quad \forall k \in [K], j \in [J]. \quad (27)$$

π_0 is the proportion of true atom null hypotheses. Random variable P with PDF $f_P(p)$ and its i.i.d. realizations $\mathcal{P} = \{p_k^{(j)}\}_{j \in [J], k \in [K]}$ represent the atom p -values

$$p_k^{(j)} = \int_{T_k^{(j)}}^{\infty} f_{T_k^{(j)} | H_k^{(j)}}(t) dt, \quad j \in [J], k \in [K] \quad (28)$$

The details on the test statistics $T_k^{(j)}$ and their PDFs under the atom null $f_{T_k^{(j)} | H_k^{(j)}}(t)$ are provided in Sec. IV-E. For now, we assume that a valid set of p -values \mathcal{P} has been observed.

Under the null hypothesis, p -values follow a uniform distribution. The distribution under the alternative may vary from atom to atom due to different levels of correlation and different probability models for the components. Thus, little is known about the exact shape of the PDF $f_{P|\overline{H}}(p_k^{(j)})$ representing those p -values $p_k^{(j)} \in \{\mathcal{P} : \overline{H}_k^{(k)} = 1\}$ where the alternative is in place.

$$f_P(p_k^{(j)}) = \pi_0 + (1 - \pi_0) \cdot f_{P|\overline{H}}(p_k^{(j)}). \quad (29)$$

The atom lfdr is $\text{lfdr}_k^{(j)}$ the posterior probability that the j th component is uncorrelated between set $k \in [K]$ and all other sets $k' \in [K] \setminus k$. Since the component null $H^{(j)}$ holds for the j th component if it is uncorrelated across all sets, the posterior probability of the component null hypotheses can be expressed through the atom lfdrs,

$$P(H^{(j)} | \mathcal{P}) = \prod_{k=1}^K \text{lfdr}_k^{(j)}. \quad (30)$$

In general, if a detector rejects a set of null hypotheses, the average probability of the null across this subset is an estimate for the resulting FDR [3]. Hence, for an activation matrix estimate $\widehat{\mathbf{M}}$, the estimated atom and component FDRs are

$$\widehat{\text{FDR}}^* = \frac{\sum_{j=1}^J \sum_{k=1}^K \widehat{M}_k^{(j)} \cdot \text{lfdr}_k^{(j)}}{\sum_{j=1}^J \sum_{k=1}^K \widehat{M}_k^{(j)}}, \quad \widehat{\text{FDR}}_{\text{cmp}}^* = \frac{\sum_{j=1}^J \mathbb{1}\left\{\sum_{k=1}^K \widehat{M}_k^{(j)} > 0\right\} \cdot \prod_{k=1}^K \text{lfdr}_k^{(j)}}{\sum_{j=1}^J \mathbb{1}\left\{\sum_{k=1}^K \widehat{M}_k^{(j)} > 0\right\}}. \quad (31)$$

In the definition of $\widehat{\text{FDR}}^*$ and $\widehat{\text{FDR}}_{\text{cmp}}^*$, we use that $\widehat{M}_k^{(j)} = 1$ whenever the atom null hypothesis $H_k^{(k)}$ is rejected. We propose to exploit this relation between lfdrs and FDRs to simultaneously control the FDRs on the atom and component level. The objective is to detect as many correlations as possible while controlling the atom and component FDRs at the respective nominal levels α and α_{cmp} . Thus, we search for the activation matrix estimate $\widehat{\mathbf{M}}^*$ with the largest number of non-zero entries such that a) the average null probability across the non-zero entries is $\leq \alpha$ and b) the average component null probability across the set of all components for which correlation between some data sets was identified is $\leq \alpha_{\text{cmp}}$. The resulting activation matrix estimator is

$$\widehat{\mathbf{M}}^* = \underset{\widehat{\mathbf{M}}}{\text{argmax}} \left\{ \sum_{j=1}^J \sum_{k=1}^K \widehat{M}_k^{(j)} : \widehat{\text{FDR}}^* \leq \alpha, \widehat{\text{FDR}}_{\text{cmp}}^* \leq \alpha_{\text{cmp}} \right\}. \quad (32)$$

To include the constraint of either none or at least two atom discoveries per row, i.e., $\sum_{k=1}^K \widehat{M}_k^{(j)} \neq 1$, we propose the following procedure. We define the *modified atom lfdr*, which replaces the smallest two atom lfdrs by their average,

$$\widetilde{\text{lfdr}}_k^{(j)} = \begin{cases} \frac{\text{lfdr}_k^{(j)} + \min_{k' \in [K] \setminus k} \text{lfdr}_{k'}^{(j)}}{2} & \text{if } k = \arg \min_{k'' \in [K]} \text{lfdr}_{k''}^{(j)} \text{ or } k = \arg \min_{k'' \in [K] \setminus k'} \text{lfdr}_{k''}^{(j)} \\ \text{lfdr}_k^{(j)}, & \text{otherwise.} \end{cases} \quad (33)$$

Then, we replace $\text{lfdr}_k^{(j)}$ in Eqs. (24), (25) by $\widetilde{\text{lfdr}}_k^{(j)}$ to obtain

$$\widehat{\text{FDR}} = \frac{\sum_{j=1}^J \sum_{k=1}^K \widehat{M}_k^{(j)} \cdot \widetilde{\text{lfdr}}_k^{(j)}}{\sum_{j=1}^J \sum_{k=1}^K \widehat{M}_k^{(j)}}, \quad \widehat{\text{FDR}}_{\text{cmp}} = \frac{\sum_{j=1}^J \mathbb{1}\left\{\sum_{k=1}^K \widehat{M}_k^{(j)} > 0\right\} \cdot \prod_{k=1}^K \widetilde{\text{lfdr}}_k^{(j)}}{\sum_{j=1}^J \mathbb{1}\left\{\sum_{k=1}^K \widehat{M}_k^{(j)} > 0\right\}}. \quad (34)$$

Then, the solution to Eq. (26) is

$$\widehat{\mathbf{M}}_{\text{MHT}} = \underset{\widehat{\mathbf{M}}}{\text{argmax}} \left\{ \sum_{j=1}^J \sum_{k=1}^K \widehat{M}_k^{(j)} : \widehat{\text{FDR}} \leq \alpha, \widehat{\text{FDR}}_{\text{cmp}} \leq \alpha_{\text{cmp}} \right\}. \quad (35)$$

Since $\widehat{\text{FDR}} \leq \widehat{\text{FDR}}^* \leq \alpha$ and $\widehat{\text{FDR}}_{\text{cmp}} \leq \widehat{\text{FDR}}_{\text{cmp}}^* \leq \alpha_{\text{cmp}}$, atom and component FDR control carries over from Eq. (32).

In practice, $\widehat{\mathbf{M}}_{\text{MHT}}$ can be determined as follows. The given set of p -values \mathcal{P} contains one p -value per atom, which quantifies the evidence that the j th component of set k is correlated with at least one other set. First compute the atom lfdrs from Eq. (27) and the modified lfdrs from Eq. (33). Sort them in ascending order. Then, find the index $m \in [K \cdot J]$ as the largest integer such that the cumulative average over the smallest m modified lfdr's is below the nominal atom FDR level α . If the m -th largest $\widetilde{\text{lfdr}}_k^{(j)}$ is equal to its corresponding atom lfdr, rejecting the null hypothesis for those atoms corresponding to the smallest m modified lfdr's guarantees that at least two discoveries per component are made. If the m -th largest modified lfdr is different from its corresponding lfdr, then

this atom is one of the atoms with the two smallest lfdrs of a component. One then has to make sure that either the null hypothesis for this second atom with one of the smallest lfdr's of that component gets rejected as well, or that none of the two get rejected.

The component FDR is estimated subsequently by averaging the component null probabilities over those components for which correlations have been identified. The resulting estimate $\widehat{\text{FDR}}_{\text{cmp}}$ is compared to the nominal component FDR level α_{cmp} . If $\text{FDR}_{\text{cmp}} \leq \alpha_{\text{cmp}}$, both atom and component FDR are controlled as desired and the estimate $\widehat{\mathbf{M}}_{\text{MHT}}$ that solves Eq. (26) has been found. If, on the other hand, $\text{FDR}_{\text{cmp}} > \alpha_{\text{cmp}}$, we iteratively remove components from the set of discoveries. In each iteration, we remove the discoveries for the component with the smallest number of atom discoveries to reduce the component lfdr while minimizing the loss in detection power on the atom level. Then, we again rank order the atom-level modified lfdrs from the remaining components for which correlation has been detected. This leaves room for additional discoveries, since the removal of discoveries for one component has also reduced $\widehat{\text{FDR}}$. The procedure terminates as soon as FDR_{cmp} falls below the nominal level α_{cmp} . The details are given in Alg. 1.

Algorithm 1 The proposed lfdr-based correlation structure detector with atom and component FDR control

Input: $\text{lfdr}_k^{(j)} \forall j \in [J], k \in [K], \alpha, \alpha_{\text{cmp}}$

Output: The activation matrix estimate $\widehat{\mathbf{M}}_{\text{MHT}}$.

- 1: Initialize $\mathcal{J}_{\text{cand}} = [J]$
 - 2: Compute all $\widetilde{\text{lfdr}}_k^{(j)}$ from Eq. (33)
 - 3: Define $|\mathcal{J}_{\text{cand}}| \cdot K$ tuples of component and set indexes $(j_\mu, k_\mu) \in \mathcal{J}_{\text{cand}} \times [K]$ s.t. $\widetilde{\text{lfdr}}_{k_\mu}^{(j_\mu)}$ is the μ th largest modified atom lfdr
 - 4: Find $m = \max \left\{ \mu \in [|\mathcal{J}_{\text{cand}}| \cdot K] : \mu^{-1} \cdot \sum_{m=1}^{\mu} \widetilde{\text{lfdr}}_{k_\mu}^{(j_\mu)} \leq \alpha \right\}$
 - 5: **if** $\widetilde{\text{lfdr}}_{k_m}^{(j_m)} \neq \text{lfdr}_{k_m}^{(j_m)}$ **then**
 - 6: **if** $\nexists \mu < m : j_\mu = j_m$ **then**
 - 7: $m = m \pm 1$ where $+$ is selected at random with probability .5
 - 8: Define the preliminary set of rejected atom null hypotheses $\overline{\mathcal{H}} = \left\{ \overline{H}_{k_\mu}^{(j_\mu)} \right\}_{\mu \leq m}$
 - 9: Find the set of component rejections $\overline{\mathcal{H}}_{\text{cmp}} = \left\{ \overline{H}^{(j)} \forall j \in \mathcal{J}_{\text{cand}} : \exists \overline{H}_k^{(j)} \in \overline{\mathcal{H}} \right\}$
 - 10: Compute $\widehat{\text{FDR}}_{\text{cmp}} = \sum_{j: \overline{H}^{(j)} \in \overline{\mathcal{H}}_{\text{cmp}}} \prod_{k=1}^K \widetilde{\text{lfdr}}_k^{(j)}$
 - 11: **if** $\widehat{\text{FDR}}_{\text{cmp}} > \alpha_{\text{cmp}}$ **then**
 - 12: Define $\nu = \min_{j: \overline{H}^{(j)} \in \overline{\mathcal{H}}_{\text{cmp}}} \sum_{k \in [K]} \mathbb{1} \left\{ \overline{H}_k^{(j)} \in \overline{\mathcal{H}} \right\}$
 - 13: Find $j^* = \arg \max_{j: \overline{H}^{(j)} \in \overline{\mathcal{H}}_{\text{cmp}}} \left\{ \prod_{k=1}^K \widetilde{\text{lfdr}}_k^{(j)} : \sum_{k \in [K]} \mathbb{1} \left\{ \overline{H}_k^{(j)} \in \overline{\mathcal{H}} \right\} = \nu \right\}$
 - 14: $\mathcal{J}_{\text{cand}} = \mathcal{J}_{\text{cand}} \setminus j^*$
 - 15: Jump to Step 3 with the remaining $\widetilde{\text{lfdr}}_k^{(j)}, k \in [K], j \in \mathcal{J}_{\text{cand}}$
 - 16: Determine the entries of $\widehat{\mathbf{M}}_{\text{MHT}}$ with $\hat{\mathbf{M}}_k^{(j)} = \mathbb{1} \left\{ \overline{H}_k^{(j)} \in \overline{\mathcal{H}} \right\} \forall k \in [K], j \in [J]$
-

So far, we have assumed that a set \mathcal{P} of p -values was provided. In the following section, we present our proposed

test statistic that extracts the evidence for correlation between components across data sets from the coherence matrix of the data.

E. The proposed test statistic

We exploit the properties of the eigenvectors of the composite coherence matrix \mathbf{C} from [1] that we summarized in Sec. III-A. Assume that $\sum_{k=1}^K M_k^{(j)} \neq 0$, i.e., there is at least one pair of sets $k, k' \in [K], k \neq k'$ such that the j th component of set k is correlated with the j th component of set k' . Then, according to [1, Theorem 2], $\mathbf{u}_k^{(j)} = \mathbf{0}_J$ if and only if $M_k^{(j)} = 0$ and $\|\mathbf{u}_k^{(j)}\|^2 = 0$. In contrast, if $M_k^{(j)} = 1$, $\|\mathbf{u}_k^{(j)}\|^2 > 0$ holds. In addition, for any eigenvector \mathbf{u} of any arbitrary matrix general, $\|\mathbf{u}\|^2 = 1$ holds.

Since the true \mathbf{C} is not available, our access is limited to the eigenvector chunks $\hat{\mathbf{u}}_k^{(j)}$ of the estimate $\hat{\mathbf{C}}$. $\hat{\mathbf{C}}$ is estimated from finite sample data and is hence subject to random estimation error. Due to this noise, its eigenvector chunks $\hat{\mathbf{u}}_k^{(j)} \neq \mathbf{0}_J \forall j \in [J], k \in [K]$ and thus also $\|\hat{\mathbf{u}}_k^{(j)}\|^2 \neq 0 \forall j \in [J], k \in [K]$. In what follows, we denote the squared estimated eigenvector chunk norm by $c_k^{(j)} = \|\hat{\mathbf{u}}_k^{(j)}\|^2$.

Theorem 1. *Consider that the j th components of all data sets are uncorrelated, i.e., $j \notin [D]$. Then, the expected value of the squared chunk norms $\mathbb{E}[c_k^{(j)}]$ is identical $\forall k \in [K]$. With $\|\hat{\mathbf{u}}^{(j)}\|^2 = 1$ follows*

$$\mathbb{E}[c_1^{(j)}] = \dots = \mathbb{E}[c_K^{(j)}] = \frac{1}{K}. \quad (36)$$

The same relation holds, if the j th components of all sets are correlated with an equal correlation coefficient.

Proof. The norm of any eigenvector of any arbitrary matrix is one. If the j th component is uncorrelated across all sets, its eigenvector $\hat{\mathbf{u}}^{(j)}$ does not exhibit a specific structure. The same holds, if j th component is equally strongly correlated across all data sets. Then, its elements follow a maximum entropy distribution with zero mean and equal variance [8], [9], i.e., they are uniformly distributed on the $J \cdot K$ -dimensional unit sphere [10]. Hence, the expected value of the J sums of distinct K entries of $\hat{\mathbf{u}}^{(j)}$ all have the same expected value and must sum to one. \square

In the examples of Fig. 2 and Fig. 3, Theorem 1 can also be observed empirically.

Conjecture 1. *Consider that the j th component of set $k \in [K]$ is correlated with the j th component of at least one other set $k' \in [K], k \neq k', j \in [J]$. $\bar{\mathcal{K}}^{(j)}$ denotes the set of all data sets whose j th components are correlated and $\mathcal{K}^{(j)}$ its complement. Then,*

$$\mathbb{E}[c_k^{(j)}] > \mathbb{E}[c_{k'}^{(j)}] \quad \forall k \in \bar{\mathcal{K}}^{(j)}, k' \in \mathcal{K}^{(j)}. \quad (37)$$

Since $\|\hat{\mathbf{u}}^{(j)}\|^2 = 1$, $\mathbb{E}[c_{k'}^{(j)}] < \frac{1}{K}$ holds for $k' \in \mathcal{K}^{(j)}$.

This conjecture follows from Theorem 1 in combination with [1, Theorem 2]. The eigenvectors of the estimated coherence matrix $\hat{\mathbf{u}}^{(j)}$ are noisy versions of the eigenvectors $\mathbf{u}^{(j)}$ of the true unavailable \mathbf{C} . For the true $\mathbf{u}_k^{(j)} = \mathbf{0}_J$ if and only if $M_k^{(j)} = 0$ and $\|\mathbf{u}_k^{(j)}\|^2 = 0$. In contrast, if $M_k^{(j)} = 1$, $\|\mathbf{u}_k^{(j)}\|^2 > 0$ holds. The chunk norms of the eigenvectors $c_k^{(j)}$ of $\hat{\mathbf{C}}$ are noisy versions of the $\|\mathbf{u}_k^{(j)}\|^2$. Conjecture 1 states that these estimates, while

not perfectly zero for uncorrelated sets, are expected to have a smaller expected value than those chunk norms associated with true correlations.

We propose to exploit these differences in the expected value of the chunk norms to identify the true correlations. Hence, we deploy the test statistic

$$\mathbb{T}_k^{(j)} = c_k^{(j)} - \mathbb{E} [c_k^{(j)}] = c_k^{(j)} - \mu_k^{(j)}, \quad \forall j \in [J], k \in [K]. \quad (38)$$

$\mu_k^{(j)}$ denotes the expectation $c_k^{(j)}$. We know that $\mu_k^{(j)} \leq \frac{1}{K}$ under the atom null hypothesis, but its exact value depends on the underlying data structure. In addition, to compute the atom p -values $p_k^{(j)}$ from Eq. (28), which are needed as inputs for our MHT correlation structure detector in Alg. 1, the PDFs $f_{\mathbb{T}_k^{(j)}|H_k^{(j)}}(t)$ under the atom null hypothesis is required for all $\mathbb{T}_k^{(j)} \forall k \in [K], j \in [J]$. The literature on the distributional properties of the spectrum of finite-sample second order statistic matrices is limited. In general, tools from random matrix theory (RMT) need to be applied. While some work on estimators for the eigenvalues and eigenvectors of random covariance matrices exist, e.g. [11], the results in the literature concerning the statistical properties of the eigenvectors are not applicable to our problem at hand. Often, the assumptions on the underlying component distributions are too restrictive [12]–[14]. The RMT overview paper [15] provides interesting insights into the distribution of the squared chunk norms under mild conditions. However, their model describes a chunk norm random variable that is marginalized over the corresponding eigenvalue magnitude. In this work, the eigenvalues are sorted such that the first eigenvector corresponds to the largest eigenvalue. The statistical properties of an eigenvector chunk norm conditioned on it being associated with the j th largest eigenvalue differ from those of an eigenvector chunk norm associated with the i th largest eigenvalue. We conclude that a general valid analytical model for distribution of the eigenvector chunk norms as utilized in this work does not exist and determining the required distributions analytically is too challenging. Instead, we resort to learning $f_{\mathbb{T}_k^{(j)}|H_k^{(j)}}(t)$ and $\mu_k^{(j)} \forall j \in [J], k \in [K]$ from the data.

F. Learning the test statistic distribution from the data

We have access to exactly one realization of each eigenvector chunk norm $u_k^{(j)}$. Thus, we deploy the bootstrap [16], [17] to obtain artificial realizations that can be used to approximate the underlying probability model. The bootstrap is a standard tool to approximate the distribution of a test statistic under the null hypothesis [18], [19] for the given number of samples. Hence, the bootstrap is not only useful for estimating theoretically unknown distributions, but can also be applied when a small sample size prohibits the use of asymptotic results [20]. The bootstrap can be deployed parametrically or non-parametrically. The former assumes a parametric data model, estimates the model parameters from the observations and then resamples from the estimated distribution. The latter resamples directly B times with replacement from the observation sample. Since little is known about shape of the distribution of the eigenvector chunk norms, we stick to the non-parametric bootstrap. The details on how we bootstrap the estimated eigenvector chunk norms are provided in Alg. 2.

G. Local false discovery rate estimation

A serious challenge when working with lfdr-based inference methods is that $f_P(p)$ is most often unavailable in practice, since the exact distribution of the p -values under the alternative cannot be specified exactly and must hence

Algorithm 2 The eigenvector chunk norm bootstrap**Input:** Observation matrices $\mathbf{X}_k \forall k \in [K]$, B **Output:** Bootstrapped squared eigenvector chunk norms $b_{\mathbf{c}_k}^{(j)*}$ *Remark:* The indices take values $j \in [J]$, $k \in [K]$, $b \in [B]$

- 1: Resample B times from the rows of \mathbf{X}_k to obtain ${}^b\mathbf{X}_k^*$
- 2: Compute ${}^b\hat{\mathbf{C}}^*$ with ${}^b\mathbf{X}_k^*$ from Eqs. (11), (9)
- 3: Find the eigenvalue decomposition (EVD) of ${}^b\hat{\mathbf{C}}^*$: $b\hat{\lambda}^{(1)*} \geq \dots \geq b\hat{\lambda}^{(JK)*}$ and $b\hat{\mathbf{u}}^{(1)*}, \dots, b\hat{\mathbf{u}}^{(JK)*}$
- 4: Compute $b_{\mathbf{c}_k}^{(j)*} = \left\| b\hat{\mathbf{u}}_k^{(j)*} \right\|^2$

be learned from the data. Methods to estimate the lfdr's from the data exist in the literature. Under the alternative, p -values closer to zero become more likely. Hence, joint p -value PDFs like $f_P(p)$ have been modeled as a mixture of a uniform and a single-parameter beta distribution component [21] or, more recently, as a mixture of multiple single-parameter beta distributions [22], [23]. In particular, the spectral method of moments-based lfdr estimator proposed in [22] and its maximum likelihood extension [23] enable accurate lfdr-based inference with FDR control even when only few handfuls of p -values are available. Thus, we deploy the lfdr estimator LFDR-SMOM-EM from [23] for estimating the lfdrs in this work.

H. The complete proposed algorithm

We present the complete **lfdr**-based **multiple hypothesis testing** procedure for complete **correlation structure** identification (LFDR-MULT-COST) in detail in Alg. 3. First, we compute the test statistics $T_k^{(j)} \forall k \in [K], j \in [J]$ under the assumption that the null hypothesis holds everywhere. Then, we bootstrap the observation matrices to obtain an estimate $\hat{F}_{T_k^{(j)}|H_k^{(j)}}(t)$ for the CDF of the test statistics under the null hypothesis. Subsequently, a p -value $p_k^{(j)}$ is computed $\forall k \in [K], j \in [J]$ to express the confidence in each local null hypothesis $H_k^{(j)}$. Then, the lfdrs are estimated. Finally, the proposed correlation structure detector from Sec. IV-C is applied. The FDR is controlled on the atom and component level, i.e., $\text{FDR} \leq \alpha$ and $\text{FDR}_{\text{cmp}} \leq \alpha_{\text{cmp}}$ while $\sum_{k=1}^K \hat{M}_j^{(k)} \neq 1 \forall j \in [J]$.

V. SIMULATION RESULTS

In this section, we numerically evaluate the performance of the proposed lfdr-based multiple testing approach to complete correlation structure identification. We simulate a variety of scenarios. Our results underline that our proposed method is very effective in identifying correlations. In particular in challenging scenarios, such as when data sets are high-dimensional and only few samples are available, it outperforms its competitors significantly in terms of detection power, while the FDR is controlled at the nominal level. We compare the proposed method's performance to the two existing approaches for multiset correlation structure identification from the literature. These are the previously summarized TSP from [1], which first estimates the number of components D correlated between at least some sets before identifying the precise sets for which correlation exists. We use equal nominal false alarm probability levels ${}_I\alpha_{\text{FA}} = {}_{II}\alpha_{\text{FA}} = 0.1$. For LFDR-MULT-COST, we present results for $\alpha = \alpha_{\text{cmp}} = 0.1$ and for

Algorithm 3 Proposed **lfdr**-based **multiple hypothesis testing** procedure for complete **correlation structure** identification (LFDR-MULT-COST)

Input: Observation matrices \mathbf{X}_k , $k \in [K]$, B , α , α_{cmp}

Output: Activation matrix estimate $\widehat{\mathbf{M}}_{\text{MHT}}$

Remark: The indices take values $j \in [J]$, $k \in [K]$, $b_0 \in [B_0]$, $b_1 \in [B_1]$

Step 1: *Computation of the chunk norms*

- 1: Compute $\widehat{\mathbf{C}}$ from Eqs. (11), (9)
- 2: Find the EVD of $\widehat{\mathbf{C}}$: $\hat{\lambda}^{(1)} \geq \dots \geq \hat{\lambda}^{(JK)}$ and $\hat{\mathbf{u}}^{(1)}, \dots, \hat{\mathbf{u}}^{(JK)}$
- 3: Divide $\hat{\mathbf{u}}^{(j)}$ into K chunks $\hat{\mathbf{u}}_k^{(j)}$
- 4: Compute $c_k^{(j)} = \left\| \hat{\mathbf{u}}_k^{(j)} \right\|^2$

Step 2: *Estimation of the distribution of the test statistic*

- 5: Obtain B bootstrapped $b c_k^{(j)*}$ from Alg. 2
- 6: Estimate $b \mu_k^{(j)*}$ by the sample means of the $b c_k^{(j)*}$
- 7: Compute the bootstrapped $b T_k^{(j)} = b c_k^{(j)*} - b \mu_k^{(j)*}$
- 8: Form the null distribution function estimates $\hat{F}_{T_k^{(j)}|H_k^{(j)}}(t)$ by sorting the bootstrapped test statistics in ascending order ${}^{(1)}T_k^{(j)} \leq \dots \leq {}^{(B)}T_k^{(j)}$

Step 3: *Computation of the test statistic*

- 9: Compute $T_k^{(j)}|H_k^{(j)}$ from Eq. (38) with $\hat{\mu}_k^{(k)}|H_k^{(k)} = \min \left[\frac{1}{B} \cdot \sum_{b=1}^B b c_k^{(j)*}, \frac{1}{K} \right]$

Step 4: *Hypothesis testing*

- 10: Compute the p -values $p_k^{(j)} = \hat{F}_{T_k^{(j)}|H_k^{(j)}}(T_k^{(j)})$
 - 11: Estimate the atom lfdrs $\text{lfdr}_k^{(j)}$ with [23, Alg. 2]
 - 12: Find the activation matrix estimate $\widehat{\mathbf{M}}_{\text{MHT}}$ with Alg. 1
-

$\alpha = .1$, $\alpha_{\text{cmp}} = 1$. While the former combination uses the widely used nominal FDR level of 0.1 for atoms and components alike, the latter combination allows for any proportion of false discoveries on the component level. Throughout our experiments, the achieved detection power is very similar for $\alpha_{\text{cmp}} = 0.1$ and $\alpha_{\text{cmp}} = 1$. Hence, the additional statistical guarantee, which increases the credibility for the identified correlation structure by controlling the FDR on the component level versus having FDR control only on the atom level comes at little cost. The second competitor originates from [24], where the underlying components are estimated via multiset canonical correlation analysis (CCA) (CCA) before each possible pair of components is tested for correlation. This results in a large number of tests if the number of data sets is large. Thus, we use a false alarm level of 0.001, as the authors of [24] suggested.

The synthetic data is generated according to the model in Eq. (4). We randomly generate orthogonal mixing matrices \mathbf{A}_k . The components in each data set have an equal variance of 1. We use both, Gaussian and Laplacian distributed components to illustrate the insensitivity of our method to the underlying data distributions. The additive noise is i.i.d. Gaussian, unless specified otherwise. The noise variance is constant across data sets and computed

from the SNR and the component variance. For the bootstrap, we use $B = 300$ resamples, which is sufficient in most applications [18].

To quantitatively evaluate the performance, we monitor the empirically obtained FDR on the atom and component level, which should both not exceed their respective nominal levels for our proposed methods. In addition, we compare the detection power of the different methods, that is, the percentage of detected true correlations, both, on the atom and the component level. Finally, we also provide some exemplary plots of the averaged estimated activation matrices $\widehat{\mathbf{M}}$ in comparison to the true activation matrix \mathbf{M} . This is useful for understanding the origin of the performance differences. We analyze the behavior in dependence of SNR, sample size, number of data sets, proportion of true correlations. In addition, we investigate the impact of outliers through ϵ -contaminated noise [25] in the Appendix A. The underlying correlation structures vary in the different experiments. All results are averaged over 100 independent repetitions.

In Experiment 1, we revisit the example from Fig. 3. $D = 6$ out of $J = 10$ components are correlated across 7, 6, 5, 4, 3 and 2 out of $K = 15$ data sets with correlation coefficients 7, .7, .65, .6, .6, .55, respectively. The correlation coefficients are constant per component, $\rho_{k,k'}^{(j)} = \rho_{k'',k'''}^{(j)} \forall k, k', k'', k''' \in [K]$.

For the remaining experiments, the correlation structure be randomized as follows. We define π_0 as the fraction of zeros in \mathbf{M} , that is, the proportion of true atom level null hypotheses among all hypotheses. Based on π_0 , D is computed such that the D th component is correlated across at least two sets. The $D - 1$ st component is correlated across one more set, the $D - 2$ nd again correlated across one more etc. The sets across which a component is correlated are selected uniformly at random. The precise value of D depends on π_0 , K and J . This randomization of the correlation allows to obtain results for a variety of different correlation structures while guaranteeing its identifiability via the coherence matrix [1]. In addition, the parameter π_0 allows to flexibly tune the sparsity of the true correlations, that is, the number of non-zero entries of activation matrix \mathbf{M} .

We define an average correlation coefficient of 0.85 for the first component with the strongest correlation and 0.5 for the D th component with the weakest correlation. The average correlation decreases linearly as $j \in [D]$ grows. We sample the correlation coefficients $\rho_{k,k'}^{(j)}$ from a Gaussian distribution with expectation $\mu_\rho = 0.85 - \frac{(0.85-0.5)}{D-1} \cdot (j-1)$ and a standard deviation $\sigma_\rho = 0.33 \cdot \frac{(0.85-0.5)}{D-1}$. The objective was to create a challenging, yet solvable scenario. We found that correlations with correlation coefficient ≤ 0.5 are barely identifiable with any of the deployed methods for the small sample sizes we consider in this work. The randomness in the value of the correlation coefficient values attributes to the real-world, where the correlation strength between the j th component of different sets may vary.

Experiment 1: In this experiment, the number of samples $N = 300$ is small. The top and bottom rows of Fig. 4a shows the performance measures on the atom and component level as a function of SNR, respectively. The atom FDR for mCCA-HT is higher than the axis limit 0.3. Such a high proportion of false discoveries makes the results of unreliable. This is also confirmed in the detection pattern for mCCA-HT on the right top of Fig. 4b for SNR = 10dB. Many false positives occur with high probability. TSP produces less false positives than mCCA-HT, but is also far more conservative, i.e., finds considerably less true correlations for SNR ≥ 5 dB. As the bottom left of Fig. 4b illustrates, this is due to an early termination in Step I. Indeed, for the displayed detection pattern with

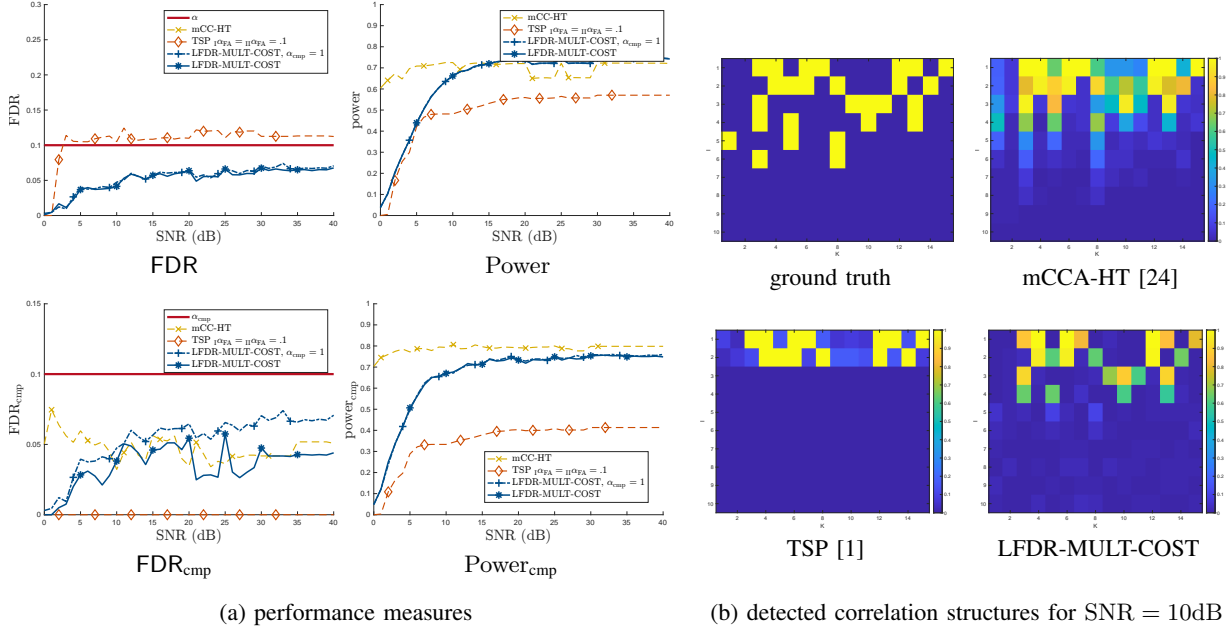


Figure 4: Experiment 1 - Performance comparison depending on the SNR. mCCA-HT exhibits an unreasonably high false discovery rate. TSP produces less erroneously detected correlations, but has low detection power for higher SNR values. Our proposed LFDR-MULT-COST fulfills its nominal FDR level while $\alpha = 0.1$ while yielding high detection power. Setting $\alpha_{\text{cmp}} = 1$ leads to slightly more false positives on the component level.

SNR = 10dB, the average number of correlated components estimated by TSP is $\hat{D} = 2$. This is far from the true $D = 6$. Hence, the error propagation from Step I to Step II causes low detection power. Our proposed LFDR-MULT-COST yields the best performance. The empirical FDR is well below the nominal level and the detection power is high. Our proposed single-step approach excels in particular for stronger signals, due to its ability to freely detect true discoveries in all components. Removing the constraint on the component level FDR by setting $\alpha_{\text{cmp}} = 1$ has little impact on the detection power. While increases the component level FDR, the empirical FDR_{cmp} remains low.

Experiment 2: The SNR = 5dB is now fixed, along $K = 20$ the number of data sets and $J = 10$ the number of components. The components and the noise are both Gaussian distributed. The proportion of true atom null hypothesis is $\pi_0 = .7$. All components are correlated between at least few sets, so there cannot be any component level false positives. Again, the atom FDR for mCCA-HT is higher than the axis limit. TSP yields a high FDR when the number of samples is small. As its corresponding detection pattern for $N = 175$ on the bottom left of Fig. 5b reveals, D is underestimated. In those components with $j \leq \hat{D}$, falsely identified correlations occur frequently. Since the small K introduces a large estimation error in the coherence matrix and thus, a lot of variation in the test statistics, our proposed method is conservative while the number of samples is small. Nevertheless, it provides highly reliable discoveries, since the FDR is controlled even for extremely small sample sizes.

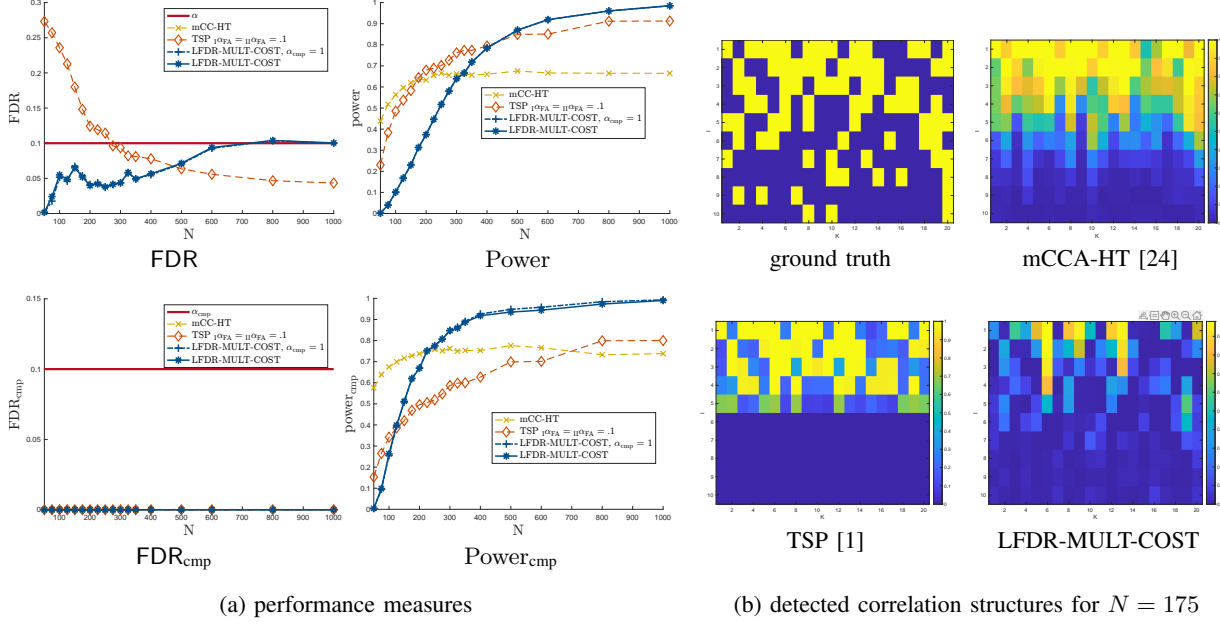


Figure 5: Experiment 2 - Performance comparison depending on the sample size. mCCA-HT yields unreasonably many false positives. TSP yields many falsely detected correlations when the sample size is very small. Our proposed LFDR-MULT-COST produces a much lower detection power, but performs consistently for all sample sizes. FDR control is maintained even at very small sample sizes. All components are correlated between at least few sets. Hence, the value of α_{cmp} has no impact.

Experiment 3: Again, SNR = 5dB and $J = 10$ components. Now, $K = 500$ is fixed and the number of data sets K varies. The components are Laplacian distributed, but the additive noise is Gaussian. The results with $\pi_0 = 0.8$ are shown in Fig. 6, additional result for $\pi_0 = 0.9$ are provided in the Appendix A.

mCCA-HT again results in a too high proportion of false positives. The discoveries of TSP contain more and more false positives, as the number of data sets K grows. Inspection of the bottom left of Fig. 6b reveals that TSP underestimates the D , preventing discoveries anywhere in components below, but commits more false positives within the first \hat{D} components than our proposed approach LFDR-MULT-COST. This is the effect discussed in Section IV-A2 of conducting many binary tests without correcting for false multiple testing, which leads to an ever increasing number of false positives when the number of tested null hypotheses increases. Our proposed method performs well, exhibiting a nearly constant atom level FDR over K and providing high detection power. The power only starts to slowly decrease when K becomes fairly large. This is due to the relative sample size: The dimensions of the coherence matrix $J \cdot K \times J \cdot K$ increase rapidly in K , while the number of available samples $N = 500$ is fixed. The effects of small sample size were discussed in Experiment 2. LFDR-MULT-COST with $\alpha_{\text{cmp}} = 1$ has a slightly increased $\text{FDR}_{\text{cmp}} > 0.1$ for $K = 9$, but yields detection power nearly identical to LFDR-MULT-COST with $\alpha_{\text{cmp}} = 0.1$. Hence, the additional component level false positive control comes at little cost.

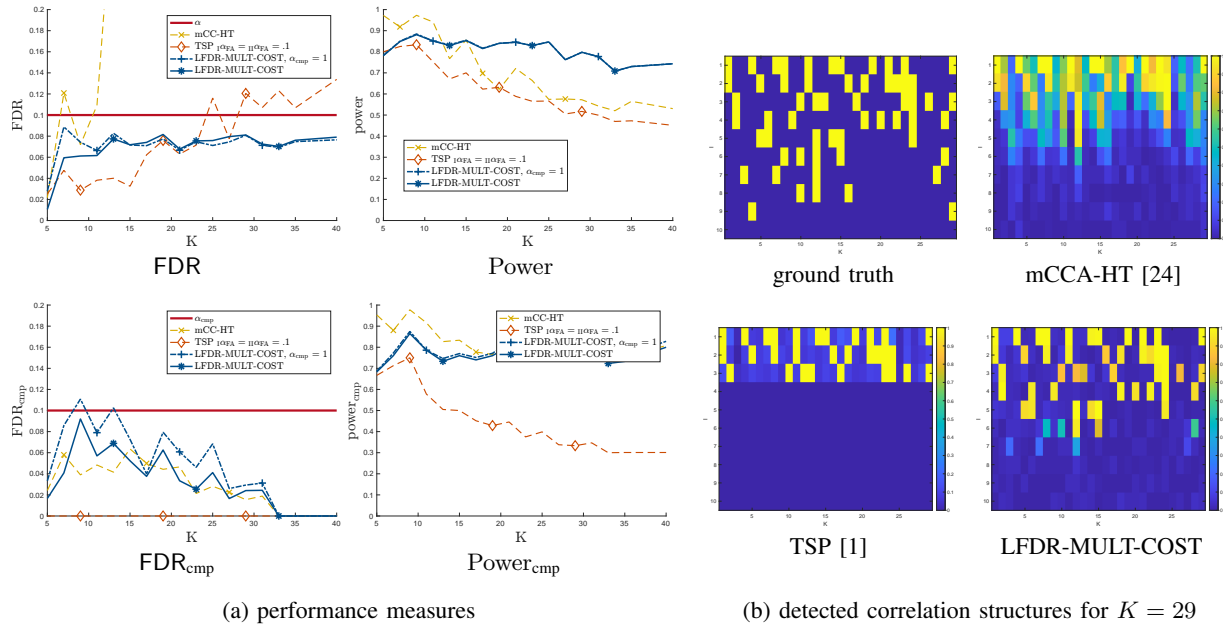


Figure 6: Experiment 3 - Performance comparison depending on the number of data sets for $\pi_0 = 0.8$. mCCA-HT yields unreasonably many false positives. The discoveries of TSP contain more and more false positives as the number of data sets grow. Hence, TSP is not well suited for applications where the number of data sets is large. The empirical FDRs for our proposed LFDR-MULT-COST are nearly constant across all K . The detection power on the atom level is constant for a while, before it starts to decline marginally. This is due to the decreasing relative sample size. Setting $\alpha_{cmp} = 1$, i.e., removing the constraint on FDR_{cmp} has little impact: As the number of sets K grows, more and more components are correlated between at least a few sets. Hence, more and more components become true positives.

Experiment 4: We now study the impact of the proportion of true atom level null hypotheses π_0 on the performance. We simulate $K = 25$ data sets with $N = 600$ samples of Gaussian components and noise, $SNR = 5dB$ and $J = 10$ components. The performance measures are shown in Fig. 7. mCCA-HT performs insufficiently. With growing π_0 , the number of true correlations decreases and maintaining a high detection power becomes increasingly difficult. The atom level detection power of our proposed LFDR-MULT-COST declines much slower than that of TSP. Remarkably, even for $.9 \leq \pi_0 \leq .975$, the detection power is only reduced on average by about 15% in comparison to the much less challenging $\pi_0 = 0.7$. Beyond $\pi_0 = .975$, also our proposed method detects nothing anymore. With LFDR-MULT-COST and $\alpha_{cmp} = 0.1$, the component level FDR is controlled everywhere. Again, the detection power on the atom level is nearly identical to the results with $\alpha_{cmp} = 1$.

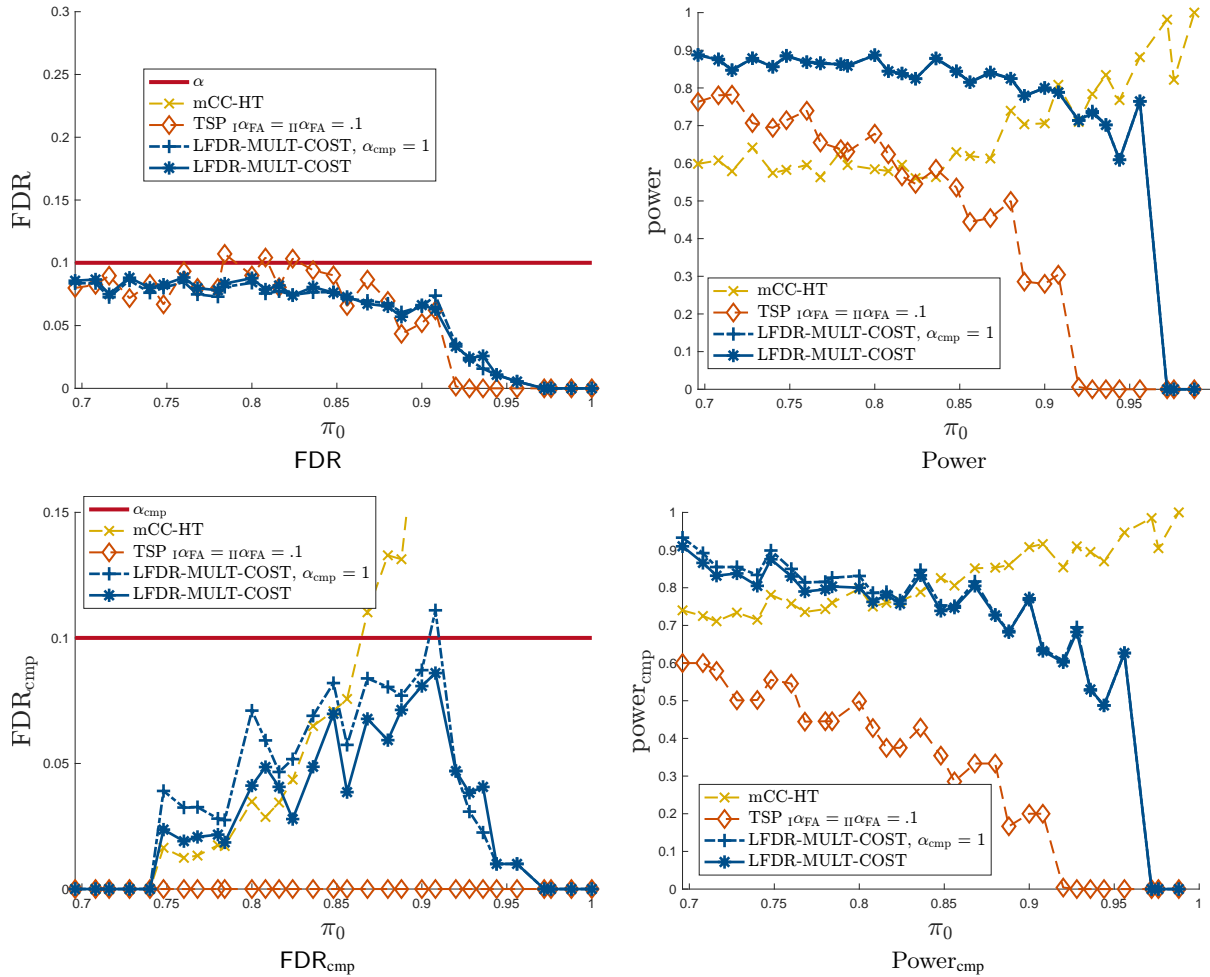


Figure 7: Experiment 4 - Performance comparison depending on π_0 . As the fraction of true positives declines, maintaining high detection power becomes increasingly challenging. mCCA-HT should not be used due to a very high atom level FDR. The detection power of our proposed LFDR-MULT-COST declines much slower than that of TSP. Hence, the proposed method is much more suitable for very challenging applications in which only a few correlations must be identified in large data sets. Again, controlling FDR_{cmp} costs close to nothing in terms of detection power. Nevertheless, it keeps FDR_{cmp} below the nominal level at all times.

VI. CONCLUSION

The problem of identifying the complete correlation structure in the components of multiple high-dimensional data sets was considered. A multiple hypothesis testing formulation of this problem was provided. The proposed solution is based on local false discovery rates and fulfills statistical performance guarantees with respect to false positives. In particular, the false discovery rate is controlled on two levels. The test statistics are based on the eigenvectors of the sample coherence matrix, whose probability models are learned from the data using the bootstrap. Our empirical results underline that our method works controls false positives even in the most challenging scenarios when sample size is very small, the number of data sets is very large, the proportion of true alternatives is very

small. In addition, it is agnostic to the underlying data and noise probability models, which makes it insensitive to distributional uncertainties and heavy-tailed noise. This makes the proposed method applicable in a large number of practical applications, such as communications engineering, climate science, image processing and biomedicine.

REFERENCES

- [1] T. Hasija, T. Marrinan, C. Lameiro, and P. J. Schreier, “Determining the dimension and structure of the subspace correlated across multiple data sets,” *Signal Process.*, vol. 176, p. 107 613, Nov. 2020.
- [2] E. Uffelmann, Q. Q. Huang, N. S. Munung, *et al.*, “Genome-wide association studies,” *Nat. Rev. Methods Primers*, vol. 1, no. 1, Aug. 2021.
- [3] B. Efron, *Large-Scale Inference: Empirical Bayes Methods for Estimation, Testing, and Prediction*. Cambridge, UK: Cambridge University Press, 2010.
- [4] J. W. Tukey, “The philosophy of multiple comparisons,” *Statist. Sci.*, vol. 6, no. 1, pp. 100–116, Feb. 1991.
- [5] Y. Hochberg and A. C. Tamhane, *Multiple Comparison Procedures*. USA: John Wiley & Sons, Inc., 1987.
- [6] Y. Benjamini and Y. Hochberg, “Controlling the false discovery rate: A practical and powerful approach to multiple testing,” *J. Roy. Statist. Soc. Ser. B*, vol. 57, no. 1, pp. 289–300, 1995.
- [7] B. Efron, “Local false discovery rates,” Tech. Rep., 2005.
- [8] L. Laloux, P. Cizeau, J.-P. Bouchaud, and M. Potters, “Noise dressing of financial correlation matrices,” *Phys. Rev. Lett.*, vol. 83, no. 7, pp. 1467–1470, Aug. 1999.
- [9] V. Plerou, P. Gopikrishnan, B. Rosenow, L. A. N. Amaral, T. Guhr, and H. E. Stanley, “Random matrix approach to cross correlations in financial data,” *Phys. Rev. E.*, vol. 65, no. 6, p. 066 126, Jun. 2002.
- [10] Z. D. Bai, B. Q. Miao, and G. M. Pan, “On asymptotics of eigenvectors of large sample covariance matrix,” *Ann. Probab.*, vol. 35, no. 4, Jul. 2007.
- [11] X. Mestre, “Improved estimation of eigenvalues and eigenvectors of covariance matrices using their sample estimates,” *IEEE Trans. on Inf. Theory*, vol. 54, no. 11, pp. 5113–5129, Nov. 2008.
- [12] P. J. Forrester and T. Nagao, “Eigenvalue statistics of the real ginibre ensemble,” *Phys. Rev. Lett.*, vol. 99, no. 5, Aug. 2007.
- [13] X. Mestre, “On the asymptotic behavior of the sample estimates of eigenvalues and eigenvectors of covariance matrices,” *IEEE Trans. Signal Process.*, vol. 56, no. 11, pp. 5353–5368, Nov. 2008.
- [14] N. J. Simm, “Central limit theorems for the real eigenvalues of large gaussian random matrices,” *Random Matrices: Theory Appl.*, vol. 06, no. 01, p. 1 750 002, Jan. 2017.
- [15] S. O’Rourke, V. Vu, and K. Wang, “Eigenvectors of random matrices: A survey,” *J. Comb. Theory Ser. A*, vol. 144, pp. 361–442, Nov. 2016.
- [16] B. Efron, *An introduction to the bootstrap*. New York: Chapman & Hall, 1994.
- [17] A. Zoubir and B. Boashash, “The bootstrap and its application in signal processing,” *IEEE Signal Process. Mag.*, vol. 15, no. 1, pp. 56–76, 1998.
- [18] A. M. Zoubir and D. R. Iskander, *Bootstrap Techniques for Signal Processing*. Cambridge University Press, Jan. 2001.
- [19] M. Gözl, V. Koivunen, and A. Zoubir, “Nonparametric detection using empirical distributions and bootstrapping,” in *Proc. 25th Eur. Signal Process. Conf.*, IEEE, Aug. 2017.

- [20] M. Gözl, M. Fauss, and A. Zoubir, "A bootstrapped sequential probability ratio test for signal processing applications," in *Proc. 2017 IEEE 7th Int. Workshop Comput. Adv. Multi-Sensor Adaptive Process.*, IEEE, Dec. 2017.
- [21] S. Pounds and S. Morris, "Estimating the occurrence of false positives and false negatives in microarray studies by approximating and partitioning the empirical distribution of p-values," *Bioinformatics*, vol. 19, pp. 1236–1242, Jan. 2003.
- [22] M. Gözl, A. M. Zoubir, and V. Koivunen, "Multiple hypothesis testing framework for spatial signals," *IEEE Trans. Signal Inf. Process. Netw.*, vol. 8, pp. 771–787, 2022.
- [23] M. Gözl, A. Zoubir, and V. Koivunen, "Estimating test statistic distributions for multiple hypothesis testing in sensor networks," in *Proc. 56th Annu. Conf. Inf. Sci. Syst.*, Mar. 2022.
- [24] T. Marrinan, T. Hasija, C. Lameiro, and P. J. Schreier, "Complete model selection in multiset canonical correlation analysis," in *Proc. 26th Eur. Signal Process. Conf.*, IEEE, Sep. 2018.
- [25] P. J. Huber and E. M. Ronchetti, *Robust Statistics*. John Wiley & Sons, Inc., Jan. 2009.

APPENDIX

In this appendix, we provide additional simulation results.

Experiment 3-b: In Fig. 8, additional for a variation of Experiment 3 from Section V are shown. Here, $\pi_0 = 0.9$. Since the proportion of true atom null hypotheses is only 10%, this is a challenging scenario. Indeed, the detection power of TSP quickly becomes problematic as K increases. Our proposed LFDR-MULT-COST proves to be more suitable in high-dimensional, highly challenging scenarios. Its detection power is nearly constant across the entire range of simulated K .

Experiment 5: We finally evaluate the robustness of the proposed method to outliers. To this end, we deploy the ϵ -contamination model [25] where a certain fraction ϵ of data samples follows a contaminating distribution. Contamination with high-powered Gaussian noise, with a standard deviation of 3 times the uncontaminated noise standard deviation was proposed in [25] in Experiment Experiment 5-a. In addition, we also evaluate the much more challenging contamination with a point mass at a fix large value in Experiment 5-b. We generate $N = 1000$ samples of $J = 6$ Gaussian components and noise vectors for $K = 12$ data sets.

a: All data sets and components get contaminated with a fraction of $\epsilon \in \{0, .25, .5, 1\}$ outliers. For $\epsilon = 0$, there is no contamination. For $\epsilon = 1$, the contaminating distribution has completely replaced the original distribution. The results are shown in Fig. 9. As we see, both TSP and LFDR-MULT-COST are fairly robust to such contamination, since the detection power and false discovery rates remain close to constant across ϵ .

b: In this experiment, we contaminate 4 out of the 6 rows in the data matrices \mathbf{X}_k for 8 out of the 12 data sets with a point mass of value 10. This is a very challenging type of outlier, since a point mass creates a strong imbalance in the tails of the contaminated noise distribution. The detection power of both methods is reduced for the contaminated data. Nevertheless, the FDR control properties of our proposed LFDR-MULT-COST remain intact, as illustrated in Fig. 10. TSP produces a higher proportion of false positives under contamination.

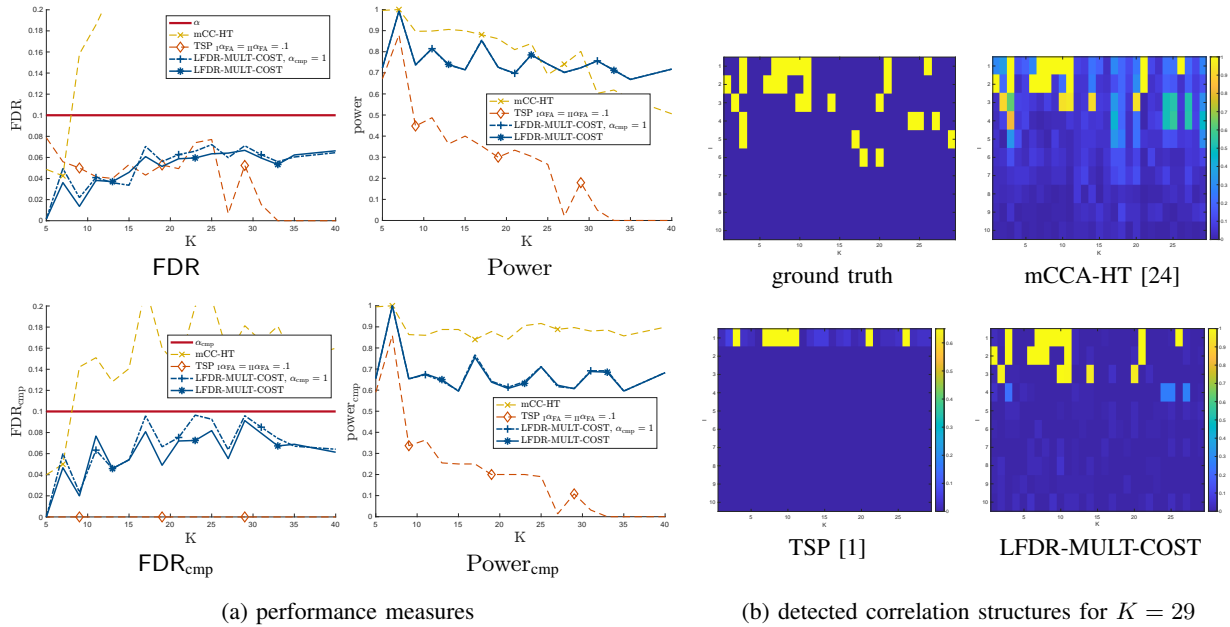


Figure 8: Experiment 3-b - Performance comparison depending on the number of data sets for $\pi_0 = 0.9$. mCCA-HT yields unreasonably many false positives. TSP has trouble identifying true correlations as the number of sets grows and as true positives become more and more sparsely distributed across the sets. The detection power with LFD-MULT-COST on the atom level declines very slowly. The decline is due to the decreasing relative sample size. Again, the control of $FDR_{\text{cmp}} \leq 0.1$ comes at no cost regarding detection power while reducing the already well-below the limit residing component FDR marginally in relation to LFD-MULT-COST with nominal level $\alpha_{\text{cmp}} = 1$.

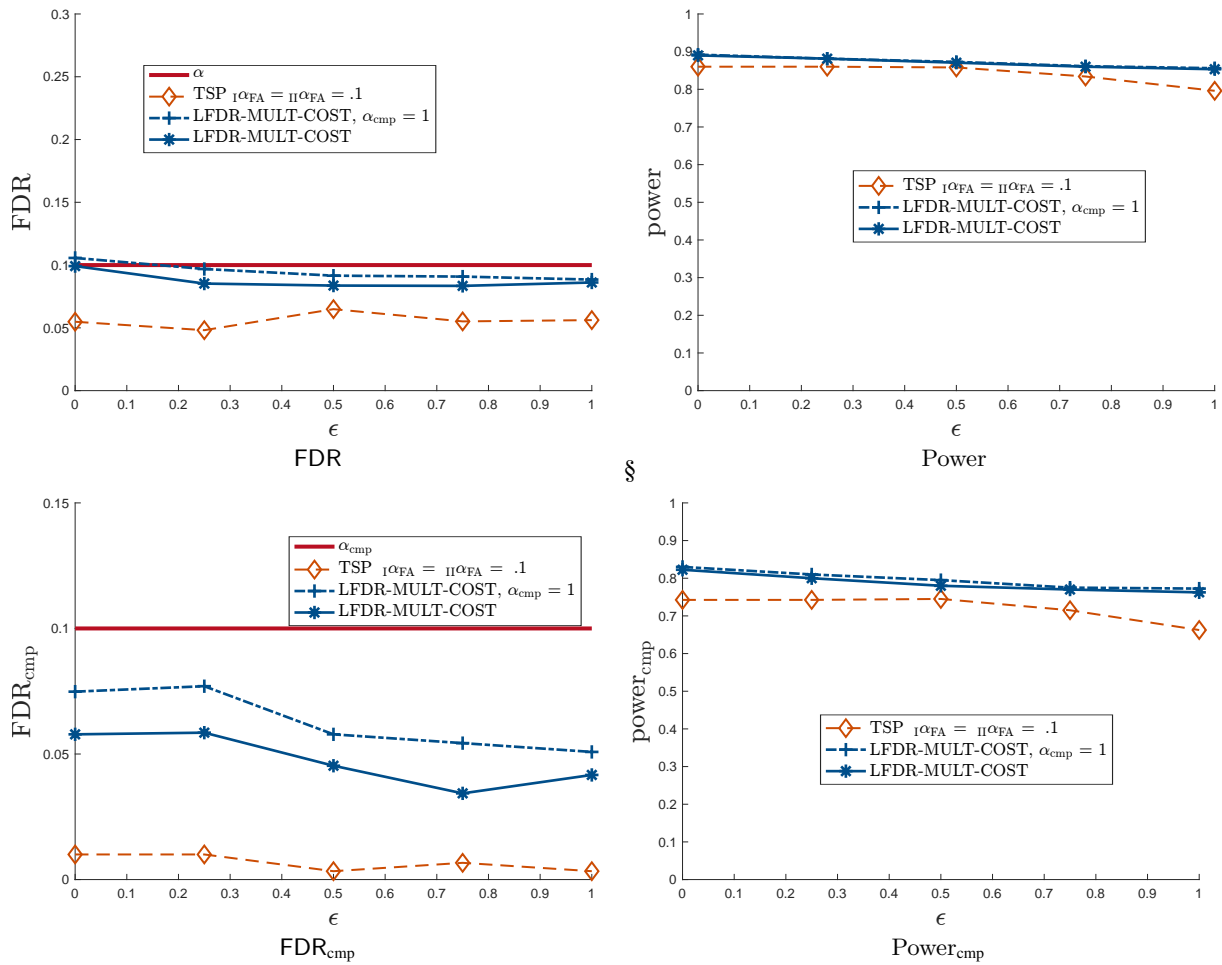


Figure 9: Experiment 5-a - Empirical evaluation of the robustness of TSP [1] and the proposed LFDR-MULT-COST with and without component-level FDR versus outliers. ϵ is the percentage of contaminated samples by an additive Gaussian contamination with large variance. All methods appear fairly robust to such outliers and yield high detection power and low FDR.

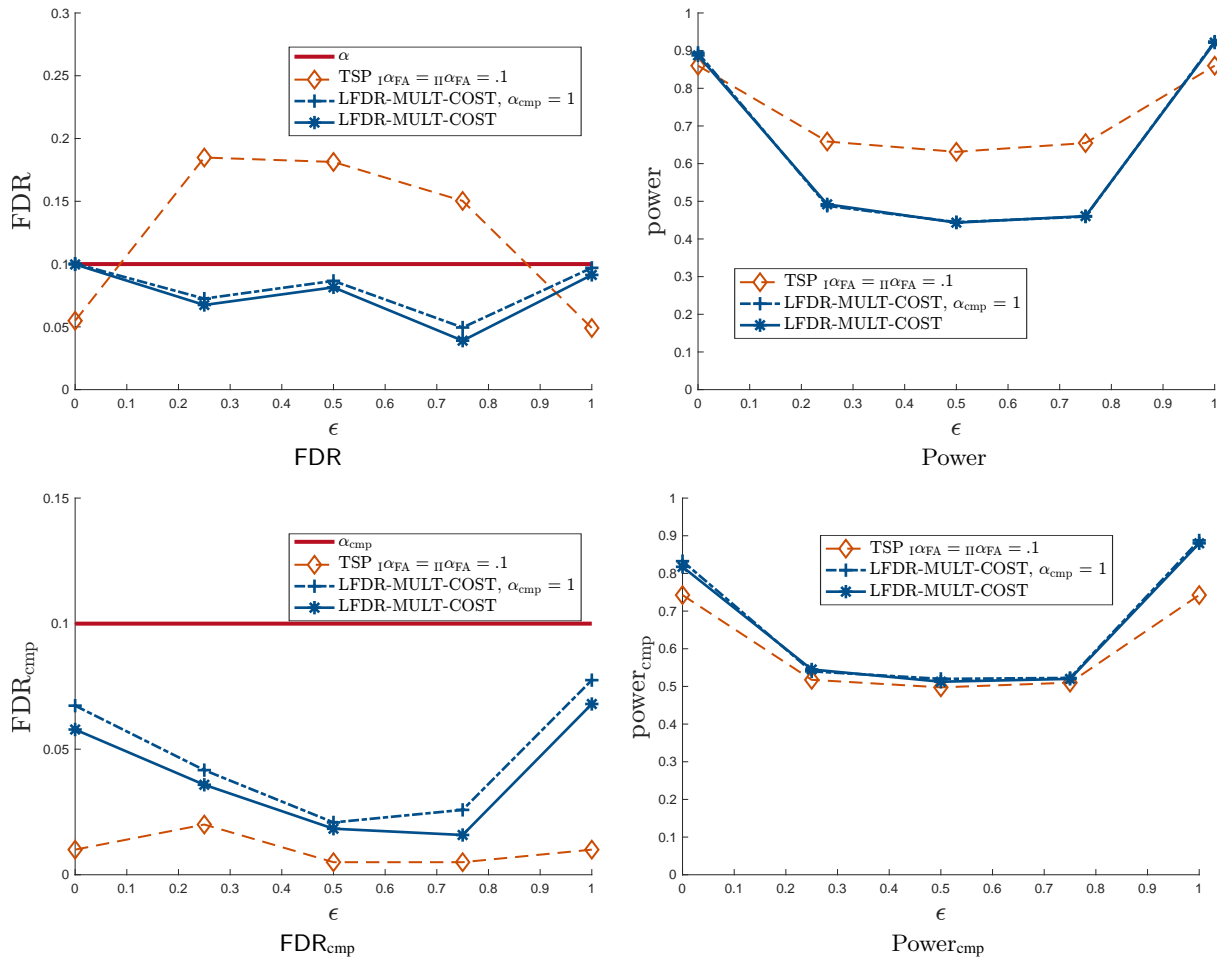


Figure 10: Experiment 5-b - Empirical evaluation of the robustness of TSP [1] and the proposed LFDR-MULT-COST with and without component-level FDR versus outliers. ϵ is the percentage of contaminated samples by an additive point mass contamination at $\delta = 10$. The FDR control of our proposed LFDR-MULT-COST is robust to this very challenging type of contamination. While the noise distribution is a mixture of the outlier point mass and the uncontaminated noise, the detection power is reduced.